

3  
4 **Post-20 Ma motion of the Adriatic plate – new constraints from**  
5 **surrounding orogens and implications for crust-mantle decoupling**  
6

7  
8 **Authors**

9 Eline Le Breton<sup>1\*</sup>, Mark R. Handy<sup>1</sup>, Giancarlo Molli<sup>2</sup>, Kamil Ustaszewski<sup>3</sup>

10 <sup>1</sup>Freie Universität Berlin, Berlin, Germany

11 <sup>2</sup>Università di Pisa, Italy

12 <sup>3</sup>Friedrich-Schiller-Universität Jena, Jena, Germany

13 \*Corresponding author: eline.lebreton@fu-berlin.de  
14

15 **Key Points**

16 - Adria has rotated  $5 \pm 3^\circ$  counter-clockwise and translated c. 110 km to the NW (azimuth  
17  $325^\circ$ ) relative to Europe since 20 Ma.

18 - Adria motion was associated with 110 km convergence relative to Moesia, 125 km in  
19 Eastern Alps and 60 km of extension in Sicily Channel.

20 - Differences between amounts of shortening and plate convergence suggest crust-mantle  
21 decoupling at active Adria-Europe boundaries.

## 22 **Abstract**

23 A new kinematic reconstruction that incorporates estimates of post-20 Ma shortening and  
24 extension in the Apennines, Alps, Dinarides and Sicily Channel Rift Zone (SCRZ) reveals  
25 that the Adriatic microplate (Adria) rotated counter-clockwise as it subducted beneath the  
26 European Plate to the west and to the east, while indenting the Alps to the north. Minimum  
27 and maximum amounts of rotation ( $2^\circ$ ,  $8^\circ$ ) are derived by using, respectively, estimates of  
28 crustal extension along the SCRZ (minimum of 30 km) combined with crustal shortening in  
29 the eastern Alps (minimum of 115 km), and a maximum amount (140 km) of convergence  
30 between Adria and Moesia across the southern Dinarides and Carpatho-Balkan orogens.  
31 When combined with Neogene convergence in the western Alps, the best fit of available  
32 structural data constrains Adria to have moved 113 km to the NW (azimuth  $325^\circ$ ) while  
33 rotating  $5 \pm 3^\circ$  counter-clockwise relative to Europe since 20 Ma. Amounts of plate  
34 convergence predicted by our new model exceed Neogene shortening estimates of several  
35 tens of kilometers in both the Apennines and Dinarides. We attribute this difference to crust-  
36 mantle decoupling (delamination) during roll-back in the Apennines and to deformation  
37 related to the northward motion of the Dacia Unit between the southern Dinarides and Europe  
38 (Moesia). Neogene motion of Adria resulted from a combination of Africa pushing from the  
39 south, the Adriatic-Hellenides slab pulling to the northeast and crustal wedging in the western  
40 Alps, which acted as a pivot and stopped further northwestward motion of Adria relative to  
41 Europe.

## 43 **1. Introduction**

44 The Adriatic microplate (Adria) is a key player in the geodynamics of the western  
45 Mediterranean because of its location between two major plates, Europe and Africa (**Fig. 1**),  
46 that have been converging since at least Late Cretaceous time [e.g., *Dewey et al.*, 1989;  
47 *Stampfli and Borel*, 2002; *Handy et al.*, 2010]. Its boundaries are highly deformed and include  
48 the Alps, Apennines, Dinarides, Hellenides and the Calabrian Arc. The Alps-Apennines and  
49 Alps-Dinarides junctions are marked by switches in subduction polarity, with Adria being the  
50 upper plate in the Alps and the lower plate in the Apennines and Dinarides [**Fig. 1**; e.g.,  
51 *Carminati and Doglioni*, 2012; *Handy et al.*, 2010; 2015b]. The Apennines have been the site  
52 of Oligo-Miocene roll-back subduction, “soft” collision and pronounced back-arc (upper-  
53 plate) extension leading to the opening of the Tyrrhenian and Liguro-Provençal Basins [**Fig.**  
54 **1**; e.g., *Royden and Burchfiel*, 1989; *Patacca et al.*, 1990; *Gueguen et al.*, 1997; *Séranne*,  
55 1999; *Faccenna et al.*, 2003; *Jolivet and Faccenna*, 2000; *Stampfli and Borel*, 2002; *Molli*,  
56 2008].

57           Reconstructing the motion of Adria remains a challenge, partly because most of it has  
58 been subducted [e.g., *Handy et al.*, 2010], but also because its eastern and western margins  
59 were very deformable [e.g., *Moretti and Royden*, 1988], making it difficult to choose stable  
60 reference points for motion studies. Adria is often considered to be a promontory of Africa  
61 and thus to have moved with Africa [e.g., *Channell and Horvath*, 1976; *Channell et al.*, 1979;  
62 *Dewey et al.*, 1989; *Mazzoli and Helmann*, 1994; *Rosenbaum et al.*, 2004; *Gaina et al.*, 2013;  
63 *Muttoni et al.*, 2013], although independent motion of Adria with respect to both Europa and  
64 Africa has been deemed necessary to explain the complex kinematics of orogenesis and basin  
65 formation in the Adriatic region [*Biju-Duval et al.*, 1977; *Dercourt et al.*, 1986]. The three-  
66 plate hypothesis has been confirmed by recent studies based on restoring shortening in the  
67 Alps, indicating that Adria's motion was intermittently independent of Africa since the onset  
68 of Adria-Europe convergence in late Cretaceous time [*Handy et al.*, 2010; 2015b].  
69 Reconstructions of the Aegean region also indicate that Adria likely moved some 40 km  
70 relative to Africa in the Pliocene [*van Hinsbergen and Schmid*, 2012]. While there is  
71 consensus that Adria's motion involved counter-clockwise (CCW) rotation with respect to  
72 Europe, the amount of rotation remains controversial. This pertains even to the Neogene part  
73 of the history during collision in the Alps, Apennines and Dinarides. Estimates of post-  
74 Paleogene CCW rotation range from a few degrees to as much as 20° depending on the  
75 authors and approach used [paleomagnetism, e.g., *Márton et al.*, 2010; *van Hinsbergen et al.*,  
76 2014a and references therein; palinspastic reconstructions, *Ustaszewski et al.*, 2008; *Handy et al.*,  
77 2010, 2015b]. The rotation pole today is generally placed within the arc of the western  
78 Alps and the western Po Basin as indicated by seismic moment [*Anderson and Jackson*, 1987]  
79 and GPS velocity studies [*Calais et al.*, 2002; *Vrabec and Fodor*, 2006; *Bennett et al.*, 2012].  
80 All of these studies assume that Adria moved as a single block, though some seismic and  
81 geodetic investigations suggest that it may have fragmented into two blocks that are currently  
82 rotating with respect to each other, as well as relative to Europe and Africa [*Oldow et al.*,  
83 2002; *D'Agostino et al.*, 2008; *Scisciani and Calamita*, 2009; *Sani et al.*, 2016].

84           This paper presents a new motion path for the Adriatic microplate since early Neogene  
85 time ( $\leq 20$  Ma). This period saw major changes in the interaction of plates in the western and  
86 central Mediterranean, and is therefore key to understanding the forces that drove plate  
87 motion [slab-pull, slab-suction, Africa-push; e.g., *Faccenna et al.*, 2004; *Handy et al.*, 2010;  
88 *Carminati and Doglioni*, 2012; *Viti et al.*, 2016] and ultimately formed the mountains and  
89 basins surrounding Adria. After reviewing the Apennines, Alps and Dinarides (section 2), and  
90 comparing existing models of Adriatic motion (section 3), we compile new estimates of

91 crustal shortening, continental subduction and extension along transects surrounding Adria  
92 (A-A'-A'', B-B', C-C', D-D' on **Fig. 1**; section 4). The information is then synthesized to  
93 provide a best-fit model of Adriatic motion that reconciles data from all neighboring orogens  
94 and basins (section 5). Finally, the motion path is used to draw inferences about the forces  
95 that drive the Adriatic plate (section 6).

96

## 97 **2. Geological setting**

98 The western Mediterranean area is a highly mobile tectonic system marked by arcuate  
99 plate boundaries with highly non-cylindrical orogens and back-arc basins (**Fig. 1**). Adria  
100 played a central role in the geodynamics of this region because of its location between two  
101 former oceans: the mid-Jurassic-early Cretaceous Alpine Tethys [e.g., *Stampfli and Borel*,  
102 2002; *Schmid et al.*, 2004; *Vissers et al.*, 2013] and the northern branch of Neotethys [e.g.,  
103 *Ricou*, 1994; *Schmid et al.*, 2008]. Today, the Adriatic microplate comprises mostly  
104 continental lithosphere [1300 km in a NW-SE direction, 250 km NE-SW and 80 km thick;  
105 *Munzarová et al.*, 2013]. It is surrounded by orogens (**Fig. 1**), from the Alps in the north  
106 where Adria is the upper plate and indents the Alpine orogenic edifice [e.g., *Schmid et al.*  
107 2004], to the Apennines and the Dinarides where Adria forms the compliant lower plate  
108 descending to the west and east, respectively [e.g., *Moretti and Royden*, 1988]. The Alps are  
109 characterized by filled to overfilled foreland basins (Molasse, Po), wholesale accretion of the  
110 lower plate including exhumed high-pressure rocks and pronounced topographic relief,  
111 whereas the Apennines and Dinarides tend to have narrow foredeeps, low-grade  
112 metamorphism of accreted lower-plate units and subdued relief [*Royden et al.*, 1987; *Royden*  
113 *and Burchfiel*, 1989].

114 Collision in the Apennines involving W-directed roll-back subduction of Adriatic  
115 continental lithosphere began no earlier than early Oligocene time [*Molli*, 2008 and references  
116 therein] as constrained by the 34-28 Ma age of rifting in the Liguro-Provençal basin  
117 [Rupelian; *Séranne*, 1999; *Jolivet et al.*, 2015] and the deposition of continental clastics in the  
118 Apenninic foredeep [Chattian-Aquitainian Macigno flysch; *Argnani and Ricci Lucchi*, 2001;  
119 *Cerrina Feroni et al.*, 2002; *Cornamusini et al.*, 2002; *Cornamusini* 2004]. Prior to collision,  
120 the polarity of subduction of the Alpine Tethys ocean is controversial; some authors favor  
121 NW-directed “Apenninic” subduction of Adria already since Late Cretaceous time [e.g.,  
122 *Jolivet and Faccenna*, 2000], whereas others invoke a switch from SE-directed “Alpine”  
123 subduction of European lithosphere to NW-directed “Apenninic” subduction of Adriatic  
124 lithosphere at about 34 Ma [e.g., *Molli*, 2008 and references therein; *Molli and Malavieille*,

125 2011 and references therein]. However, the polarity of pre-Neogene subduction is not  
126 important for the purposes of this paper, which focuses on post-20 Ma motion of Adria.

127 The Apennines continue into the Calabrian Arc, where the lithosphere of the Ionian  
128 Sea forming the southernmost part of the Adriatic microplate is actively subducting beneath  
129 Europe (**Fig. 1**). *Faccenna et al.* [2001] proposed that the Calabrian Arc formed in late  
130 Miocene time in response to slab tearing during the advanced stages of slab roll-back, back-  
131 arc extension and opening of the Tyrrhenian Sea. The nature of the lithosphere beneath the  
132 Ionian Abyssal Plain (**Fig. 1**) remains controversial, with oceanic [e.g., *de Voogd et al.*, 1992;  
133 *Speranza et al.*, 2012] or hyper-extended continental lithosphere [e.g., *Hieke et al.*, 2003]  
134 proposed so far. However, the length and retreat of the slab under the Calabrian arc and  
135 Tyrrhenian Sea suggest that the downgoing lithosphere connected to the Ionian lithosphere is  
136 oceanic. Moreover, numerous geophysical studies showed that the 330-km wide [*Catalano et*  
137 *al.*, 2001] Ionian Basin has a 7-9 km thick oceanic crust [*Cowie and Kuznir*, 2012] of Early  
138 Mesozoic age [220-230 Ma; *Speranza et al.*, 2012] covered by more than 5 km of Meso-  
139 Cenozoic sediments [*de Voogd et al.*, 1992; *Cowie and Kuznir*, 2012]. We will return to this  
140 point below, as it has implications for whether Adria was a rigid promontory of Africa or an  
141 independent plate during the convergence of Africa and Europe.

142 The amount of shortening in the Apennines is poorly constrained despite the  
143 abundance of seismic data collected over the years. Previous studies estimated shortening by  
144 assuming that orogenic shortening during roll-back subduction was compensated entirely by  
145 upper-plate extension in the Liguro-Provençal basins, amounting to zero convergence  
146 between Adria and Europe [*Faccenna et al.*, 2001]. This resulted in estimates of upper-plate  
147 extension (and thus also of maximum orogenic shortening) of 240 km and 780 km,  
148 respectively, for northern and southern transects of the Apennines (Gulf of Lion to the  
149 northern Apennines via Corsica, and Gulf of Lion to Calabria via Sardinia; *Faccenna et al.*,  
150 2001, their Figure 1]. Although the shortening estimate for the southern transect appears to  
151 coincide with the length of the slab anomaly extending to the NW from the Calabrian Arc  
152 [e.g., *Piromallo and Morelli*, 2003], there is no reason to assume a priori that Apenninic  
153 shortening was equal to extension. Moreover, studies suggested that the mantle lithosphere  
154 subducting beneath the Apennines delaminated from the crust [e.g. *Channell and Mareschal*,  
155 1989; *Serri et al.*, 1993; *Chiarabba et al.*, 2009, 2014; *Benoit et al.*, 2011]. Delamination  
156 [*Bird*, 1979] involves peeling off of the lithospheric mantle from the crust and does not  
157 necessarily entail an equivalent amount of crustal shortening as the lithospheric mantle sinks  
158 into the asthenosphere.

159 The Alps contain the sutured remains of Alpine Tethys [e.g., *Stampfli et al.*, 1998;  
160 *Schmid et al.*, 2004; *Handy et al.*, 2010], which opened as an arm of the North Atlantic in two  
161 stages, from 170-131 Ma (Piemont-Liguria Basin) and 131 to 93 Ma [Valais Basin; *Frisch*  
162 1979; *Stampfli and Borel*, 2002; *Schmid et al.*, 2004]. Closure of Alpine Tethys occurred  
163 during NNW convergence of Adria with Europe between 84 Ma and 35 Ma [*Handy et al.*,  
164 2010]. Collision in the Alps involved SE-directed subduction of the European margin and was  
165 punctuated by detachment of the European slab at 35-30 Ma [*von Blanckenburg and Davies*  
166 1995; *Schmid et al.*, 2004]. This led to crustal wedging and indentation beginning at about 30  
167 Ma and 23-21 Ma, respectively, in the western and eastern Alps [*Handy et al.*, 2015b and  
168 references therein]. The difference in the amount of Neogene indentation along strike of the  
169 Alps is directly related to the rotation of Adria, a point to which we return below.

170 The Dinarides are a SW-vergent fold-and-thrust belt (**Fig. 1**), most of which formed  
171 during Late Jurassic to early Oligocene time by the progressive closure of the northern branch  
172 of Neotethys (Meliata-Maliac-Vardar ocean) and subsequent collision and deformation of the  
173 NE Adriatic margin [e.g., *Pamić et al.*, 1998; *Babić et al.*, 2002; *Schmid et al.*, 2008;  
174 *Ustaszewski et al.*, 2010]. The part of the history relevant to this paper began with detachment  
175 of the NE-dipping Adriatic slab, triggering calc-alkaline magmatism in the Dinaric nappe pile  
176 in late Eocene-early Miocene time [37-22 Ma; *Schefer et al.*, 2011]. From Late Oligocene  
177 onward, thrusting and folding propagated to the SW into the foreland [e.g., *Tari*, 2002; *Roure*  
178 *et al.*, 2004], accompanied by dextral strike-slip faulting [*Picha*, 2002; *Kastelić et al.*, 2008].  
179 The amount of shortening in the Dinarides is poorly constrained at present. Neogene upper-  
180 plate extension in the Dinarides [*Matenco and Radivojević*, 2012] is minor compared to the  
181 amount of upper-plate extension in the Pannonian Basin [*Ustaszewski et al.*, 2008] and  
182 Apennines cited above. Extension in the Pannonian Basin occurs in the upper plate of the  
183 zero-convergence Carpathian system [*Royden and Burchfiel*, 1989] and therefore has little  
184 effect on the relative motion of Adria and Europe studied here. In the next section, we review  
185 the main unresolved problems with existing kinematic models of Adria as a prelude to the  
186 new approach used in this study.

187

### 188 **3. Existing reconstructions of Adriatic plate motion**

189 The classical approach for reconstructing plate motion is to assume that tectonic plates  
190 are rigid, then apply Euler's theorem to describe their rotation on an ideally spherical Earth by  
191 fitting magnetic anomalies and fracture zones in oceanic basins, or using paleomagnetic  
192 studies on continents [e.g., *Morgan*, 1968; *Le Pichon et al.*, 1977]. The quality of the

193 magnetic database has improved over recent decades to the point where the motions of major  
194 plates such as Europe and Africa are reasonably well constrained [e.g., *Dobrovine and*  
195 *Tarduno*, 2008; *Seton et al.*, 2012]. However, this approach is inadequate to reconstruct the  
196 motion of Mediterranean microplates like Adria, whose oceanic portions have been almost  
197 entirely subducted (**Fig. 1**; section 2) or do not have oceanic anomalies of Miocene age  
198 [Ionian Sea; *Speranza et al.*, 2012].

199 The idea that Adria was a rigid promontory of Africa since at least Jurassic time [e.g.,  
200 *Channell et al.*, 1979; *Rosenbaum et al.*, 2004; *Speranza et al.*, 2012] and moved together  
201 with Africa since that time [e.g., *Dewey et al.*, 1989; *Capitanio and Goes*, 2006; *Gaina et al.*,  
202 2013] is based primarily on paleomagnetic studies indicating little or no rotation of Adria with  
203 respect to Africa [e.g., *Channell et al.*, 1979; *Channell*, 1996; *Rosenbaum et al.*, 2004].  
204 However, recent paleomagnetic studies on stable parts of Adria (Adige embayment, Istria and  
205 Apulia, **Fig. 1**) indicate that Adria may have rotated CCW by as much as 20° relative to  
206 Africa since about 20 Ma [*Márton*, 2003; *Márton et al.*, 2008; 2010; 2011; *van Hinsbergen et*  
207 *al.*, 2014a]. Also, recent magnetic studies suggest that the Ionian crust is oceanic [e.g.,  
208 *Speranza et al.*, 2012] with a continuous lithospheric mantle between the northern margin of  
209 Africa and Italy [e.g., *Catalano et al.* 2001; *Mele*, 2001; *Rosenbaum et al.*, 2004], implying  
210 that Adria has been ‘rigidly’ connected with Africa since Triassic time [age of the oceanic  
211 crust, 220-230 Ma; *Speranza et al.*, 2012]. However, Neogene SW-NE striking thrusts and  
212 positive inversion structures in the Ionian abyssal plain [*Gallais et al.*, 2011; *Polonia et al.*,  
213 2011; *Roure et al.*, 2012] are interpreted as reactivated normal and transform faults originally  
214 formed at spreading centers of the Ionian Sea [*Gallais et al.*, 2011]. These structures indicate  
215 that the crust beneath the Ionian Sea is not rigid, but deformable. Moreover, several NW-SE  
216 trending rifts opened during Miocene time along the African Margin in the Sicily Channel  
217 Rift Zone [SCRZ, **Fig 1**; e.g. *Civile et al.*, 2008; 2010]. These structures both in the Ionian  
218 Sea and along the African Margin are therefore evidence for possible relative motion of Adria  
219 away from Africa in Neogene time.

220 Moreover, plate motion models invoking Adria as a rigid promontory of Africa are  
221 unable to account adequately for the opening and closure of Alpine Tethys, as discussed in  
222 Handy et al. [2010]. For one, the E-W and N-S dimensions of Alpine Tethys in such models  
223 [e.g., *Capitanio and Goes*, 2006] do not corroborate available estimates of N-S convergence  
224 in the Alps [*Schmid et al.*, 1996; *Handy et al.*, 2010; 2015b]. Either the N-S length of Alpine  
225 Tethys was smaller than deduced from such models, and/or the Adriatic microplate moved

226 independently of the African plate [*Biju-Duval et al.*, 1977; *Dercourt et al.*, 1986] for at least  
227 part of the period considered above.

228 To test the different models of Adria motion with respect to Europe, we use the  
229 compilation of finite rotations of *Gaina et al.* [2013] for Africa based on a best-fit of magnetic  
230 anomalies in the Atlantic, and of *Seton et al.* [2012; using paleomagnetic studies of *Speranza*  
231 *et al.*, 2002] for the Corsica-Sardinia block that best fit the amount and timing of spreading in  
232 the Liguro-Provençal Basin (see also section 4.2). We also tested the model of *Handy et al.*  
233 [2015b] that accounts for shortening in the Alps and proposes independent motion of Adria  
234 relative to Africa. All plate reconstructions and rotation calculations in this paper are  
235 performed with GPlates software [*Boyden et al.*, 2011]. Independent motion of Adria is  
236 supported by present-day GPS velocities [e.g. *D'Agostino et al.*, 2008] and by the  
237 aforementioned extension along the African Margin - and therefore motion of Adria away  
238 from Africa - in Neogene time [*SCRZ; Civile et al.*, 2008; 2010].

239 For the past 20 Ma, motion of Adria together with Africa (**Fig 2**, in green) would  
240 necessitate 170 km of NW-SE directed Neogene convergence in the western Alps, which far  
241 exceeds current estimates of Neogene shortening in the western Alps, including the recent  
242 estimate of c. 30-40 km of *Schmid et al.* [2017] obtained from areal balancing of lithospheric  
243 cross sections. It even exceeds the 113 km convergence estimate that *Handy et al.* [2015b]  
244 obtained by retro-deforming the Alpine nappe stack in map view, a value that they regarded  
245 as an absolute maximum (see also section 4.3). Adria moving together with Africa also calls  
246 for 35 km and 65 km of Neogene overall convergence along NE-SW transects in the northern  
247 Apennines and southern Dinarides-Carpatho-Balkan respectively, which both seem plausible.

248 The discrepancy between measured and model-based shortening estimates in the  
249 western Alps can only be resolved if Adria is assumed to have moved independently of  
250 Africa. We note that the model of *Handy et al.* [2015b] uses Neogene shortening in the  
251 southern Alps to obtain a CCW rotation of Adria relative to Europe of some 20°, which would  
252 require far too much Neogene convergence in the southern Dinarides-Carpatho-Balkan (350  
253 km, **Fig. 2**, in red) and an implausible 330 km of Neogene extension in the Ionian Sea and/or  
254 African Margin. None of these large estimates are supported by available geological data.  
255 Therefore, data from the other surrounding orogens (Apennines and Dinarides) and basins  
256 (western Mediterranean basins and SCRZ) are needed to better constrain the Neogene motion  
257 and amount of CCW rotation of Adria relative to Europe.

258

#### 259 **4. New constraints on post-20 Ma Adria motion**



260 To constrain the motion of Adria in Neogene time, we choose 4 transects along which  
261 to estimate convergence and divergence of Adria relative to Europe, Corsica and Africa (**Fig.**  
262 **1, sections 4.1-4.4**): (1) **southern France - Corsica - northern Apennines** (Transect A-A'-  
263 A'') perpendicular to rifting and spreading of the Liguro-Provençal Basin, and parallel to the  
264 CROP03 seismic profile [*Alberti et al.*, 1998; *Barchi et al.* 1998a, 1998b, 2003; *Decandia et*  
265 *al.*, 1998]. We choose this transect because upper-plate extension is modest and shortening  
266 can be better estimated than in the southern Apennines; (2) **western (Ivrea) and eastern Alps**  
267 (Transect C-C') where recent restorations are available [*Handy et al.*, 2010, 2015b; *Schmid et*  
268 *al.*, 2017]; (3) **southern Dinarides-Carpatho-Balkan** (Transect B-B'), where seismic  
269 tomography [UU-P07 model from *Amaru*, 2007; *Hall and Spakman*, 2015] and industrial  
270 active-source seismic data [*Bega* 2013, 2015] are available to estimate the amount of  
271 subducted lithosphere since Oligocene-early Miocene slab breakoff and Miocene crustal  
272 shortening, respectively, and where Miocene Pannonian extension is modest [*Matenco and*  
273 *Radivojević*, 2012]; (4) **Africa - southern Italy** (Transect D-D'), perpendicular to the  
274 Pantelleria Rift, the main rift of the SCRZ.

275 It is important to note that estimates of crustal shortening along these transects only  
276 correspond to convergence of the Adriatic and European plates if the crust and lithospheric  
277 mantle moved coherently during orogeny. Plate convergence is defined here as the decrease in  
278 distance between points on undeformed parts of the upper and lower plates of the orogen.  
279 Where mantle delamination, intracrustal decoupling or tectonic erosion have occurred, the  
280 amount of crustal shortening recorded by folding and thrusting will be less than the amount of  
281 plate convergence. As discussed below, these processes all occurred, sometimes together, so  
282 that most shortening values below provide minimum estimates of Adria-Europe convergence.  
283 Irrespective of the processes at active margins, shortening estimates in fold-and-thrust belts  
284 are almost always minima due to erosion of the hangingwall tiplines of thrusts and/or footwall  
285 cutoffs.

286

#### 287 **4.1. Extension vs. shortening in the northern Apennines (Transect A-A'-A'')**

288 In the Apennines, contemporaneous Neogene shortening and upper-plate extension  
289 were estimated separately to arrive at an overall amount of deformation parallel to A-A'-A''.  
290 The amount of upper-plate extension was estimated by constructing a crustal-scale profile  
291 along transect A-A'-A'' from a recent map of Moho depth [*Spada et al.* 2013, their Figure 11],  
292 and from topography and bathymetry [global model ETOPO1 of *Amante and Eakins*, 2009].  
293 This involved first removing the 55-km length of oceanic lithosphere (spreading) in the

294 central part of the Liguro-Provençal Basin [Jolivet *et al.*, 2015] from transect A-A' and 100-  
295 km length at the NE end of transect A'-A'', where Adria is the downgoing plate (**Fig. 3a**). The  
296 profile was then restored to an assumed pre-extensional crustal thickness of 30 km, as  
297 preserved beneath southern France (**Fig. 3b**). However, the crust beneath Corsica and Italy  
298 was orogenically thickened prior to the onset of upper-plate extension [Jolivet *et al.*, 1998;  
299 Faccenna *et al.*, 2001], as evidenced by Eocene high-pressure metamorphism exhumed in the  
300 footwalls of Alpine thrusts reactivated as Miocene normal faults on Alpine Corsica [e.g.,  
301 Martin *et al.*, 2011 and references therein] and in some Tuscan units of the northern  
302 Apennines [Massa unit and along-strike equivalents; e.g., Theye *et al.*, 1997; Molli *et al.*,  
303 2000; Bianco *et al.*, 2015]. We have therefore assumed an orogenically thickened crust of 40  
304 km (**Fig. 3b**), in agreement with the present Moho depth in the central Apennines [Spada *et al.*  
305 *et al.*, 2013] where the orogenic crust is not deepened by downward pull of the Adriatic slab.

306 This results in a total of  $223 \pm 30$  km of upper-plate extension along transect A-A'-A''  
307 (**Fig. 3**), which can be divided into  $61 \pm 16$  km of rifting from 34-21 Ma [age of syn-rift  
308 sediments; Seranne, 1999; Jolivet *et al.*, 2015], 55 km of sea-floor spreading from 21-16 Ma  
309 [age of post-rift sediments and CCW rotation of the Corsica-Sardinia block; Seranne, 1999;  
310 Jolivet *et al.* 2015; Speranza *et al.*, 2002; Seton *et al.*, 2012] in the Liguro-Provençal Basin,  
311 and  $107 \pm 14$  km of extension in the Tyrrhenian Sea from 16-0 Ma [age of syn-rift sediments;  
312 Seranne, 1999; Jolivet *et al.*, 2015]. The large uncertainties reflect the large variation in Moho  
313 depths along the section [Spada *et al.*, 2013; their Figure 11]. Note that if the initial thickness  
314 of crust beneath Corsica and Italy was assumed to be only 30 km, the amount of extension in  
315 the Tyrrhenian Sea (A'-A'') would be only  $51 \pm 18$  km instead of  $107 \pm 14$  km. This would in  
316 turn yield an average of  $77 \pm 44$  km extension. However, we favor the  $107 \pm 14$  km value  
317 which is based on the estimates of orogenic crustal thickness beneath Corsica and Tuscany  
318 prior to extension, as explained above. Moreover, our total estimate of  $223 \pm 30$  km Oligo-  
319 Miocene extension is in good agreement with the 240 km of total extension that Faccenna *et al.*  
320 *et al.* [2001] obtained for the same transect and time period.

321  
322 Shortening is difficult to estimate in the northern Apennines due to contractional  
323 reactivation of pre-orogenic normal faults as thrusts [e.g. Tavarnelli *et al.*, 2001] and to  
324 subsequent extensional reactivation of these thrusts during roll-back subduction [e.g. Brogi  
325 and Liotta, 2006]. This makes tectonostratigraphic markers unreliable for estimating thrust  
326 displacement. Early attempts to estimate shortening in the Umbria-Marche belt of the northern  
327 Apennines assumed a thin-skinned thrusting with detachment at the sediment-basement

328 interface, yielding up to 100 km of shortening [Bally *et al.*, 1986; Lavecchia *et al.*, 1987;  
329 Calamita and Deiana., 1988; Calamita *et al.*, 1990]. However, more recent studies using  
330 active-source seismic data from the CROP-03 profile invoked a thick-skinned thrusting  
331 involving the basement and multiple detachment levels, resulting in conservative shortening  
332 estimates ranging from 30 to 60 km (average  $45 \pm 15$  km) [Barchi *et al.*, 1998b; Alberti *et al.*,  
333 1998; Coward *et al.*, 1999; Tavarnelli *et al.*, 2004; Mazzoli *et al.*, 2005; Butler *et al.*, 2006].  
334 Shortening in the Umbria-Marche belt initiated in Burdigalian time [c. 20 Ma, Barchi *et al.*,  
335 1998b] as constrained by the age of syn-orogenic foredeep sediments (Marnoso Arenacea  
336 Fm). Older foredeep sediments of Oligo-Miocene age (c. 34 – 20 Ma, Macigno Fm) are  
337 preserved in Tuscany in the western “Tyrrhenian” segment of the CROP03 transect, where all  
338 orogenic structures are overprinted by upper-plate extension [Barchi *et al.*, 1998a; Decandia  
339 *et al.*, 1998; Brogi and Liotta, 2006]. However, pre-20 Ma sediments and structures are not  
340 directly relevant for the post-20 Ma aforementioned shortening estimates.

341 To summarize,  $107 \pm 14$  km of post-20 Ma upper-plate extension exceeded an average  
342 of  $45 \pm 15$  km of coeval orogenic shortening, resulting in a possible overall divergence of  
343 about  $62 \pm 29$  km along transect A'-A” (Fig. 4). However, shortening estimates can  
344 underestimate plate convergence considerably. Moreover, if we perform the same calculation  
345 with the whole range of possible values for both shortening (30-100 km) and extension ( $77 \pm$   
346  $44$  km) along transect A'-A”, we end up with an overall divergence of  $10.5 \pm 80.5$  km, with  
347 an uncertainty higher than the mean value. In light of this poor constraint, independent  
348 estimates of shortening and extension are needed from the other surrounding orogens and  
349 basins.

350

#### 351 **4.2. Neogene convergence in the southern Dinarides-Carpatho-Balkan (transect B-** 352 **B')**

353 The external part of the Dinarides accommodated only minor Mio-Pliocene shortening  
354 ( $\leq 20$  km) according to reflection seismic profiles interpreted from off- and onshore industry  
355 data in southern Montenegro and northern Albania [Bega 2013, 2015]. Miocene and younger  
356 shortening across the orogenic front increases to some 80-100 km as one moves to the  
357 southeast into the Tirana foredeep basin of central Albania [Schmid *et al.*, 2014]. This along-  
358 strike change in shortening has been attributed to a SE increase in the contribution of Hellenic  
359 roll-back subduction [Handy *et al.*, 2014, 2015a]; the Neogene component of this roll-back  
360 subduction was accommodated by a combination of post-middle Miocene CCW block  
361 rotation and orogen-parallel extension limited to southeast of the Shkoder-Peja Normal Fault

362 (SPNF, **Fig. 1**), as documented by paleomagnetic studies [*Kissel et al.*, 1995] and structural  
363 work [*Handy et al.*, 2014, 2015a]. Thus, for the purposes of this paper, we only regard  
364 Neogene shortening north of the SPNF, where effects of Hellenic rollback subduction are  
365 negligible.

366 Neogene opening of the Pannonian Basin in the upper plate of the neighboring  
367 Carpathian orogen involved no convergence between Adria and Europe [*Royden and*  
368 *Burchfiel*, 1989] and therefore had little, if any, effect on our estimates of Adria-Europe  
369 convergence in the southern Dinarides-Carpatho-Balkan. Moreover, our transect B-B' crosses  
370 south of the Pannonian Basin where Neogene extension amounts to less than 10 km based on  
371 the geometry of Mio-Pliocene rift basins in the seismic interpretation of *Matenco and*  
372 *Radivojević* [2012; their Fig. 4].

373 Out-of-sequence thrusting in the internal Dinarides [e.g. *Ustaszewski et al.*, 2008] and  
374 strike-slip faulting east of the Sava Suture [Timok Fault, *Fügenschuh and Schmid*, 2005] also  
375 occurred along this transect, the latter during the Neogene northward motion of the Dacia Unit  
376 around the Moesian promontory of Europe and escape into the Pannonian embayment behind  
377 the eastwardly retreating Carpatho-Balkan orogen. The lack of reliable markers precludes  
378 quantifying the effect of strike-slip faulting, but given the range of rotations of the Tisza and  
379 Dacia units [16-38° clockwise, *Ustaszewski et al. 2008* and references therein], the overall  
380 Adria-Europe (Moesia) convergence was significantly more, perhaps on the order of a 100  
381 km, than Neogene shortening in the external Dinarides.

382 An absolute maximum on the amount of Adria-Europe (Moesia) convergence along  
383 our transect B-B' is given by the length (140 km) of a positive P-wave velocity anomaly  
384 imaged in seismic tomography [model UU-P07 of *Amaru 2007*; *Hall and Spakman*, 2015;  
385 **Fig. 5**]. This can be interpreted as the Adriatic slab dipping beneath the Dinarides;  
386 unfortunately, neither the age, the detachment depth, nor the exact location of the slab with  
387 respect to the surface geology are known. Slab break-off in the Dinarides occurred between  
388 about 37 and 22 Ma as inferred from the distribution of calc-alkaline magmatism [*Schefer et*  
389 *al.*, 2011]. In light of the minor Mio-Pliocene crustal shortening in the external Dinarides,  
390 most of this truncated slab length probably accrued during Paleogene Adria-Europe  
391 convergence, for which there is abundant geological evidence in the Dinarides [e.g., *Schmid et*  
392 *al.*, 2008].

393

394 **4.3. Western (Ivrea) and Eastern Alps (transect C-C')**

395           Adria-Europe convergence in the western Alps is difficult to ascertain because  
396 shortening varies around the arc of the western Alps and partly preceded arcuation [*Collombet*  
397 *et al.*, 2002; *Schmid et al.*, 2017]. At the SW end of the arc in the Ligurian Alps, the arcuation  
398 was accentuated by eastward rollback subduction of the northern Apennines and  
399 counterclockwise rotation of the Corsica-Sardina block [*Vignaroli et al.*, 2008]. We  
400 considered the approaches of *Handy et al.* [2015b] and *Schmid et al.* [2017] which entail  
401 different assumptions and yield different amounts of Neogene convergence (113 km) and  
402 shortening (30-40 km) estimates, respectively. Adria-Europe convergence in the Western  
403 Alps is defined here as displacement of the city of Ivrea (in the Ivrea Zone) on an undeformed  
404 part of Adria relative to a point on stable Europe in the Alpine foreland (the Schwarzwald of  
405 southern Germany). *Handy et al.* [2015b] retrodeformed the Alpine thrusts in map view using  
406 previously published estimates of shortening (their Fig. A1) and maintaining compatibility  
407 around the arc by avoiding overlaps in thrusts during stepwise restoration. Their 113 km of  
408 post-20 Ma, Adria-Europe convergence along an azimuth of 325° is a maximum estimate  
409 because restoring thrust displacements orthogonally to differently oriented thrust tip lines  
410 within the arc leads to a space problem. The authors solved this by translating Adria by an  
411 amount greater than the shortening measured along individual cross sections around the arc.  
412 Recently, *Schmid et al.* [2017] obtained a shortening estimate of about 30-40 km from areally  
413 balanced lithospheric cross sections around the arc. However, this estimate must be regarded  
414 as a minimum for Neogene Adria-Europe convergence due to erosion of thrusts tip lines and  
415 cutoffs, as well as possible tectonic erosion within the orogen. We also note that any obliquity  
416 of the convergence vector to the trend of the thrust belts around the western Alpine arc would  
417 result in shortening estimates less than the overall Europe-Adria convergence [*Lacassin,*  
418 1987]. The 30 and 113 km estimates therefore very broadly bracket the actual amount of  
419 Neogene Adria-Europe convergence in the Western Alps.

420

421           In the eastern Alps, post-20 Ma shortening along transect C-C' amounts to a minimum  
422 of 115 km, comprising 65 km [*Linzer et al.* 2002] and 50 km [*Schönborn, 1999*], respectively,  
423 north and south of the Periadriatic fault. However, shortening along this transect probably  
424 does not represent the entire amount of Adria-Europe convergence, some of which was  
425 accommodated by eastward, orogen-parallel extrusion of orogenic crust in the Tauern  
426 Window [e.g., *Scharf et al.*, 2013; *Favaro et al.*, 2017]. Approximately 150 km of continental  
427 subduction can be deduced from the length of the +Vp slab anomaly imaged beneath the  
428 eastern Alps [*Handy et al.*, 2015b, their Figure B3] though this is only a crude estimate due to

429 the highly variable, drop-like shape of this slab in the tomographic images of *Lippitsch et al.*  
430 [2003]. We consider this 150-km amount of subduction as an absolute upper limit on the  
431 amount of Adria-Europe Neogene convergence; therefore, post-20 Ma Adria-Europe  
432 convergence along transect C-C' ranges from 115 to 150 km.

433

#### 434 **4.4. Sicily Channel Rift Zone (transect D-D')**

435 The continental margin between Africa and Sicily was stretched by a series of NW-  
436 SE trending rifts that developed along the Sicily Channel Rift Zone (SCRZ, **Fig. 1**) during  
437 Neogene time [e.g. *Jongsma et al.*, 1987; *Argnani* 1990; *Corti et al.*, 2006; *Civile et al.*, 2008;  
438 2010]. This area shows evidence for both extension in the SCRZ (100 km wide) and dextral  
439 transtension along the Malta Escarpment [**Fig. 1**; 3 km vertical relief over 200 km length;  
440 *Jongsma et al.*, 1987; *Dogliani et al.*, 2001]. The reason(s) for this extension are unclear; it  
441 may have accommodated shortening in the Maghreb chain, rollback of the Calabrian slab  
442 [*Argnani* 1990] or be related to a change in the rheology of the northern African continental  
443 lithosphere [*Civile et al.*, 2010]. Here, we propose that this extension accommodated the  
444 divergence between Adria and Africa during the post-20 Ma CCW rotation of Adria. The  
445 overall amount of extension is still poorly constrained. A crustal profile perpendicular to the  
446 main rift of the SCRZ (Pantelleria Rift, south of Sicily) and parallel to our transect D-D' (**Fig.**  
447 **1**) was published by *Civile et al.* [2008, their Figure 9] based on their interpretation of the  
448 CROP seismic lines M-25. The amount of NE-SW extension obtained from balancing this  
449 section for an initial thickness of 25 km (present-day thickness on both side of the rift) is  
450 about 30 km. Taking into account the other rifts along the SCRZ and the transtensional  
451 deformation along the Malta Escarpment, we consider this 30 km of extension to represent the  
452 minimum amount of Neogene divergence of Africa and Adria (D-D').

453

#### 454 **5. Post-20 Ma motion and rotation of Adria relative to Europe**

455 Combining amounts of extension, shortening and subduction obtained above from the  
456 orogens and basins surrounding Adria (section 4, **Table 1**) allows us to place tighter  
457 constraints on Adria-Europe and Adria-Africa motion. To describe the rotation of Adria, we  
458 choose an axis at the aforementioned city of Ivrea [*Handy et al.*, 2010, 2015b] due to its  
459 location at the northwesternmost stable part of Adria (**Fig. 1**) and its general coincidence with  
460 the Miocene-to-recent rotation axis for Adria proposed in previous geodetic and geophysical  
461 studies [e.g. *Vrabec and Fodor*, 2006; *D'Agostino et al.*, 2008; *Ustaszewski et al.*, 2008].  
462 However, we emphasize that the Ivrea rotation axis is not the finite Euler rotation pole for

463 Adria as a whole because Ivrea has undergone translation relative to Europe since 20 Ma  
464 together with Adria; therefore, the finite rotation pole for Adria is a combination of both the  
465 motion of Ivrea/Adria and the rotation of Adria about the Ivrea axis (**Fig. 6**).

466 We test two plate-motion scenarios utilizing either (1) the 113 km of Adria-Europe  
467 convergence in the Western Alps discussed above [*Handy et al.*, 2015b] or (2) a smaller  
468 amount of 60 km [closer to the minimum shortening estimate of *Schmid et al.*, 2017]. For  
469 both scenarios, we run a series of tests that account for different amounts of rotation, from 4°  
470 clockwise to 20° counter-clockwise (**Fig. 6; Appendix 1**). For each such test, we calculate the  
471 amounts of Adria-Europe divergence/convergence along transects A-A'-A'', B-B', C-C' and  
472 D-D', and compare them with data in section 4 in order to obtain a best-fit model for post-20  
473 Ma Adria motion (**Table 1; Appendix 1**).

474

475 The post-20 Ma motion of Adria relative to Europe along transect A-A'-A'' is divided  
476 into two components: (1) the motion of Corsica relative to Europe (transect A-A'); and (2) the  
477 motion of Adria relative to Corsica (transect A'-A''). As mentioned in section 4.1, 55 km of  
478 sea-floor spreading occurred between 21 and 16 Ma [*Seranne* 1999; *Speranza et al.* 2002;  
479 *Gattacceca et al.*, 2007; *Jolivet et al.*, 2015] in the Liguro-Provençal basin along transect A-  
480 A' (**Fig. 3**). This necessitates a CCW rotation of the Corsica-Sardinia block relative to Europe  
481 as already demonstrated in paleomagnetic studies [e.g., *Speranza et al.*, 2002; *Gattacceca et*  
482 *al.*, 2007]. For a constant spreading rate of 11 km/Ma, Corsica moved about 44 km away from  
483 Europe between 20 and 16 Ma along transect A-A'. This is identical within error to the 40 km  
484 of Corsica-Sardinia motion predicted along the same transect by *Seton et al.* [2012; Euler pole  
485 and rotation angle from *Speranza et al.*, 2002; **Fig. 4**]. A more recent model for the Corsica-  
486 Sardinia block [*Advokaat et al.*, 2014 based on *Gattacceca et al.*, 2007 for Neogene time]  
487 predicts less than 20 km of post-20 Ma displacement of Corsica along transect A-A'. We  
488 believe this underestimates the actual amount of spreading [c. 40 km according to *Jolivet et*  
489 *al.*, 2015] and therefore use the *Seton et al.* [2012] plate motion model for the motion of  
490 Corsica-Sardinia.

491 Post-20 Ma motion of Adria (A'') relative to Corsica (A') was associated with some  
492  $107 \pm 14$  km of extension in the Tyrrhenian Sea and Tuscany as shown above and in **Figure**  
493 **4**. During the same period, a minimum of  $45 \pm 15$  km shortening was accommodated in the  
494 northern Apennines (section 4.1). Assuming that this shortening represents the minimum  
495 convergence, we obtain an overall maximum divergence of  $62 \pm 29$  km between Adria (A'')  
496 and Corsica (A). To accommodate this overall divergence, Adria would have rotated at most

497 15.5 ± 4° CCW (11 to 19.5° CCW) relative to Europe given 113 km of convergence in the  
498 western Alps (Model 1), or 14.75 ± 4.25° CCW (10.5 to 19° CCW) for only 60 km of  
499 convergence in the western Alps (Model 2). Using the same approach but with the largest  
500 uncertainties in our data (77 ± 44 km of extension and 65 ± 35 km shortening along A'-A'';  
501 Section 4.1 and Table 1), the range of maximum rotation of Adria relative to Europe increases  
502 to 7.75 ± 11.75° (4° CW to 19.5° CCW, Model 1; 4.5° CW to 19° CCW for Model 2;  
503 **Appendix 1**).

504 If the observed Neogene shortening in the southern external Dinarides (c. 20 km along  
505 transect B-B'; Section 4.2 and Table 1) represents the true amount of Adria-Europe (Moesia)  
506 convergence, then rotation of Adria was negligible, if at all existent (0.6° CW for Model 1,  
507 0.3° CCW for Model 2; **Table 1 and Appendix 1**). In contrast, using the 140-km slab-  
508 anomaly length (**Fig. 5**) as a maximum of Adria-Europe (Moesia) convergence would yield  
509 maximum CCW rotation of Adria of 7° CCW for Model 1 and 8° CCW for Model 2. In the  
510 eastern Alps (transect C-C'), 115-150 km of Adria-Europe convergence corresponds to a  
511 CCW rotation of Adria ranging from 6.5 ± 3° (Model 1) to 14 ± 3° (Model 2). A minimum of  
512 30 km divergence between Adria and Africa across the Sicily Rift Zone (SCRZ, transect D-  
513 D') corresponds to a minimum CCW rotation of Adria of 3.5° for Model 1 and 4° for Model  
514 2. Therefore, no rotation of Adria – as required for only 20 km of convergence in the southern  
515 external Dinarides - would not fit the data in the eastern Alps and SCRZ. Additional  
516 convergence along B-B' related to strike-slip faulting and northward motion of Dacia into the  
517 Pannonian embayment (section 4.2) therefore fits well with the kinematic constraints imposed  
518 by the other orogens surrounding the Adriatic Plate.

519 Using 60 km of convergence in the western Alps (Model 2) requires much more CCW  
520 rotation of Adria (14 ± 3°) to fit the data in the Eastern Alps which in turn requires far too  
521 much convergence in the southern Dinarides-Carpatho-Balkan (240 ± 50 km; Fig. A9 of  
522 Appendix 1) and too much divergence between Adria and Africa (215 ± 55 km; Fig. A11 of  
523 Appendix 1). Therefore, the best fit to all the available data involves convergence according  
524 to Model 1 in the western Alps (113 km; Step 1 in **Fig. 6**) and CCW rotation of Adria of 5.25  
525 ± 1.75° about the Ivrea axis (Step 2 in **Fig. 6, Table 1**). The error associated with all our  
526 reconstructions and measurements amounts to 10 km, corresponding to 0.5-1.5° of rotation,  
527 depending on the distance to the rotation pole. Thus, the CCW rotation of Adria that fits all  
528 the available data is 5 ± 3° about the Ivrea axis. The mean value corresponds to a CCW  
529 rotation of 5.35° about a finite Euler rotation pole located in Spain at 38.20°N, 3.16°W.

530



## 531 6. Discussion

### 532 6.1. Assessing the model

533 The range of CCW Adria rotation of  $5 \pm 3^\circ$  is within error of the  $9.8 \pm 9.5^\circ$  CCW  
534 rotation proposed by *van Hinsbergen et al.* [2014a] based on their paleomagnetic study of the  
535 Apulian peninsula, southern Italy (**Fig. 1**), but much less than the  $20^\circ$  previously obtained  
536 from shortening values in the southern Alps [*Ustaszewski et al.*, 2008; *Handy et al.*, 2015b].  
537 These shortening estimates come from near the Ivrea rotation axis in the western part of the  
538 southern Alps [Bergamasche Alps, 70 km of *Schönborn*, 1992] where some of the shortening  
539 attributed to the Neogene may actually be older [e.g. *Doglioni and Bosellini*, 1987; *Fantoni et*  
540 *al.*, 2004]. Certainly, applying  $20^\circ$  of CCW rotation to the entire Adriatic plate can be ruled  
541 out on the grounds that it would require far too much Neogene convergence in the southern  
542 Dinarides-Carpatho-Balkan and Neogene extension in the Ionian Sea (**Fig. 2**).

543 In a test of different plate scenarios for Adria, *van Hinsbergen et al.* [2014a]  
544 concluded that either Neogene shortening in the western Alps has been underestimated by as  
545 much as 150 km or Neogene extension in the Ionian Basin has been underestimated by as  
546 much as 420 km. However, Neogene shortening in the western Alps certainly does not exceed  
547 113 km of convergence [our Model 1; section 4.3; *Handy et al.*, 2015b], an amount that is  
548 much greater than usually proposed for shortening in the western Alps [c. 30-40 km; *Schmid*  
549 *et al.*, 2017]. If one assumes only 60 km of convergence (our Model 2), then this would  
550 require  $14 \pm 3^\circ$  of CCW Adria rotation to fit the data in the eastern Alps, implying too much  
551 convergence in the southern Dinarides-Carpatho-Balkan and too much divergence along the  
552 SCRZ (Section 5 and Table 1). Obviously, this is strongly dependent on the location of the  
553 rotation pole for Adria; here, we used the city of Ivrea for our first reconstruction step (section  
554 5; **Fig. 6**). The rotation pole may have changed through time but this was not tested in this  
555 study. We recall that using another rotation pole such as that for Africa relative to Europe (so  
556 that Adria would move together with Africa) would require far too much convergence in the  
557 Western Alps (170 km, **Fig. 2**).

558 Our proposed best-fit CCW Adria rotation of about  $5^\circ$  relative to Europe calls for  
559 about 60 km of post-20 Ma NE-SW directed extension between Africa and Adria, which is  
560 much less than the 420 mentioned by *van Hinsbergen et al.* [2014a]. The actual amount of  
561 extension accommodated there is difficult to assess because most of the Ionian lithosphere  
562 was subducted beneath the advancing Calabrian and Hellenic arcs in Pliocene time [e.g.,  
563 *Malinverno and Ryan*, 1986; *Royden*, 1993; *Faccenna et al.*, 2003; *Gutscher et al.*, 2016];  
564 only a small triangular patch of the Ionian abyssal plain remains unsubducted (**Fig. 1**).

565 Seismic profiles of this remnant basin indicate Neogene tectonic inversion along NE-SW  
566 striking thrust faults rather than extensional deformation [*Gallais et al.*, 2011; *Polonia et al.*,  
567 2011; *Roure et al.*, 2012]. However, Neogene NE-SW directed extension along the SCRZ  
568 [e.g. *Civile et al.*, 2008] and right-lateral transtension along the Malta Escarpment [e.g.  
569 *Jongsma et al.*, 1987; *Dogliani et al.*, 2001] on the African Margin of the Ionian Sea (**Figs. 1**  
570 **and 7**) accommodated the southeastward advance of the Calabrian Arc [e.g., *Jongsma et al.*,  
571 1987; *Frizon de Lamotte et al.*, 2011; *Roure et al.*, 2012] and most likely the NE-SW  
572 divergence of Adria and Africa (section 4.4; **Fig. 7**). In sum, evidence of Neogene NW-SE  
573 directed extension along the African margin of the Ionian Sea is compatible with the NE-SW  
574 divergence of Adria and Africa as featured in our best-fit model for CCW Adria rotation.  
575 More data from the SRCZ are needed to refine this model.

576 A possible solution to the dilemma above is that the Adriatic plate fragmented, with  
577 the northern part rotating independently of the southern part [*Oldow et al.*, 2002; *D'Agostino*  
578 *et al.*, 2008; *Sani et al.*, 2016]. Indeed, seismic reflection profiling (CROP M15), GPS  
579 velocities and diffuse seismicity in the central Adriatic Sea have been interpreted as evidence  
580 for NW-SE striking thrusts and dextral strike-slip faults along the so-called Mid-Adriatic  
581 Ridge or MAR [**Fig. 1**; *Scisciani and Calamita*, 2009]. If we split Adria into two blocks along  
582 the MAR and move the northern block as in our best-fit model and the southern block  
583 together with Africa, the resulting deformation along the MAR would be 50-100 km  
584 (eastwardly increasing) of dextral strike-slip with a transtensional component ( $\leq 10$  km of  
585 extension) to accommodate CCW rotation of the northern block relative to the southern block.  
586 However, the structures imaged along CROP M15 transect are only contractional and/or  
587 transpressive; there is no evidence for transtension or for 50-100 km of dextral strike-slip  
588 deformation [*Scisciani and Calamita*, 2009]. In order to allow simultaneous Neogene CCW  
589 rotation of Adria relative to Europe and independent motion of Adria relative to Africa, the  
590 Ionian Sea and/or its adjacent margins must have accommodated Neogene extension.

591

## 592 **6.2. Discrepant shortening and convergence as evidence for crust-mantle** 593 **decoupling?**

594 The best-fit CCW Adria rotation of about  $5^\circ$  relative to Europe entails c. 8 km of  
595 overall Adria-Europe convergence in the northern Apennines (A-A'-A''), c. 110 km of across  
596 the southern Dinarides-Carpatho-Balkan (B-B''), 113 km of convergence in the western Alps  
597 (Ivrea), c. 125 km of convergence in the eastern Alps (C-C') and c. 60 km of divergence  
598 between Africa and Adria (D-D''). Predicted Adria-Europe convergence in the best-fit model

599 exceeds measured shortening in all three orogens surrounding the Adriatic plate. These  
600 discrepancies tell us something about mechanisms of orogeny in the circum-Adriatic  
601 mountain belts.

602 Continental roll-back subduction in the northern Apennines involved nearly zero  
603 Adria-Europe convergence, with about  $115 \text{ km} \pm 14 \text{ km}$  of continental subduction if we use  
604 the  $107 \text{ km} \pm 14 \text{ km}$  of extension obtained by areal balancing (section 4.1). This would be  
605 close to the amount of crustal shortening obtained from the ‘thin-skinned’ interpretations (c.  
606  $100 \text{ km}$ , section 4.1), but far greater than the favored ‘thick-skinned’ interpretations ( $30\text{-}60$   
607  $\text{km}$ , section 4.1). We attribute this deficiency of crustal shortening to tectonic erosion and/or  
608 to lithospheric and lower crustal delamination in the Apennines.

609 Likewise, the discrepancy between observed Miocene crustal shortening and inferred  
610 Adria-Europe (Moesia) convergence along transect B-B’ implies wholesale vertical  
611 decoupling. The zone of decoupling is most probably located between the Dinarides and the  
612 Moesia promontory of Europe, where arcuate strike-slip faults [e.g., Timok Fault of  
613 *Fügenschuh and Schmid*, 2005] accommodated Miocene northward extrusion and clockwise  
614 rotation of the Dacia part of the Tisza-Dacia Unit [e.g. *Ustaszewski et al.*, 2008].

615

### 616 **6.3. Possible forces driving Adriatic motion in Neogene time**

617 Neogene motion of the Adriatic plate raises the question of its driving forces, indeed,  
618 of whether its motion was at all independent of that of the larger plates. Certainly, pull of the  
619 slab beneath the Apennines can be ruled out as a driving force because the Adriatic plate  
620 rotated CCW to the NE, i.e., away from the westward direction of its subduction beneath  
621 Europe. Likewise, pull of an Adriatic slab segment beneath the eastern Alps is probably  
622 negligible due to its limited length [ $\leq 150 \text{ km}$  in the eastern Alps, *Lippitsch et al.*, 2003]. So  
623 far, P-wave tomography shows no evidence of a slab anomaly in the northern Dinarides  
624 [*Wortel and Spakman*, 2000; *Piromallo and Morelli*, 2003], precluding a component of slab  
625 pull to the NE.

626 This leaves eastward pull of the Adriatic slab beneath the northwestern Hellenides  
627 and/or northward push of the African plate as the only viable drivers of post-20 Ma Adria  
628 motion (**Fig. 7**). P-wave tomography has shown that the Hellenic slab descends through the  
629 Mantle Transitional Zone into the lower mantle [*Piromallo and Morelli*, 2003; *van*  
630 *Hinsbergen et al.*, 2005]. Similar directions (to the NW) and rates [ $7 \text{ mm/yr}$ ; *Gaina et al.*,  
631 2013 for Africa and our best-fit model for Adria] of motion of Adria and Africa relative to  
632 Europe during Neogene time indicate that Adria was pushed to the northwest by Africa, as

633 proposed by *Handy et al.* [2010, 2015b]. However, the northwestward motion of Adria most  
634 likely slowed – if not stopped – as Adria indented and wedged in the western Alps along the  
635 Ivrea Body [*Handy and Zingg, 1991; Zingg et al., 1990; Schmid et al., 2017*]. Then, pull of  
636 the NE-dipping slab beneath the northwestern Hellenides, to which the eastern part of the  
637 Adriatic plate was (and still is) attached, drove the CCW rotation of Adria and divergence  
638 from Africa, while the Apenninic-Calabrian trench retreated rapidly. Today, the remaining  
639 Adriatic plate is squeezed between Europe and Africa while the latter still pushes to the north.  
640 In response to that push, Adria most likely started to fragment internally, as indicated by the  
641 present-day seismicity and deformation within Adria [*Oldow et al., 2002; D’Agostino et al.,*  
642 *2008; Scisciani and Calamita, 2009; Sani et al., 2016*].

643 In summary, we propose that Adria’s northward motion in Neogene time was driven  
644 by Africa’s advance, while the CCW rotation of Adria resulted from a combination of  
645 wedging of its rigid northwestern end in the western Alps and northeastward pull of the  
646 Adriatic slab descending beneath the northwestern Hellenides. This left Adria's eastern edge  
647 free to swing northeastward, out of the way of Africa

648

## 649 **7. Conclusions**

650 Neogene motion of the Adriatic plate is key to understand how contrasting orogenic  
651 styles develop within the same overall convergent tectonic regime. This study provides a new  
652 post-20 Ma motion path for the Adriatic microplate that fits available geological and  
653 geophysical data from the Alps, Apennines, Dinarides and Sicily Channel Rift Zone (SCRZ).  
654 During the last 20 Ma, upper-plate extension ( $107 \pm 14$  km) has exceeded shortening (c. 30-60  
655 km) in the northern Apennines, while Adria subducted beneath the southern Dinarides (> 20  
656 km) and indented both the western Alps (c. 30-113 km) and eastern Alps (c. 115-150 km).  
657 The best-fit for Adria motion is a CCW rotation relative to Europe of c.  $5^\circ$  about a finite Euler  
658 rotation pole located in Spain at  $38.20^\circ\text{N}$ ,  $3.16^\circ\text{W}$ . This motion calls for almost no overall  
659 Neogene Adria-Europe convergence in the northern Apennines, 113 km in the western Alps,  
660 125 km in the eastern Alps, and 110 km between Adria and Moesia, mostly across the  
661 Carpatho-Balkan orogen. Furthermore, the estimated divergence between Africa and Adria of  
662 60 km was accommodated by extension along the SRCZ and dextral transtension along NW-  
663 SE striking transform faults (Malta escarpment).

664 Plate convergence exceeds crustal shortening in all orogens surrounding Adria. We  
665 attribute this difference to tectonic erosion and crust-mantle decoupling of the Adriatic  
666 lithosphere, expressed differently in the three orogens: (1) delamination during roll-back in

667 the Apennines; (2) northward motion of the Dacia Unit between the Dinarides and Europe  
668 (Moesia); and (3) eastward lateral extrusion of the Tauern Window in the Eastern Alps during  
669 northward indentation of Adria into Europe.

670 The main driving force of Adria motion was a push from Africa to the northwest until  
671 the Adriatic plate slowed and stopped as it indented Europe in the western Alps. Then the  
672 main force was a pull to the east by the slab beneath the northwestern Hellenides. This  
673 triggered a slight CCW rotation of Adria relative to Europe and divergence from Africa. As  
674 Africa still pushes to the north, the Adriatic plate most likely started to fragment internally as  
675 documented by GPS and seismic studies cited above.

676

### 677 **Supporting information**

678 Appendix 1 presents the results of the two series of tests for Model 1 and Model 2 of post-20  
679 Ma amount of Adria rotation. Appendix 2 (Movie S1) is an animated map-reconstruction of  
680 the western Mediterranean based on our favored Model 1 (5.35° CCW rotation about a finite  
681 Euler rotation pole located at 38.20°N, 3.16°W).

682

### 683 **Acknowledgments**

684 We acknowledge financial support of the German Research Foundation (DFG; BR 4900/2-1,  
685 HA 2403/16-1 and US 100/4-1). We thank Wim Spakman for kindly providing the  
686 tomographic slice across the Dinarides, as well as Douwe van Hinsbergen and Enrico  
687 Tavarnelli for their thorough reviews. In addition, this work benefited greatly from  
688 stimulating conversations with Andrea Brogi, Claudio Faccenna, Edi Kissling, Domenico  
689 Liotta, Giorgio Minelli, Stefan Schmid and Martina Zucchi. The data supporting this paper  
690 are available in the supporting information and references, or by contacting the first author.

691

### 692 **References**

693

- 694 Advokaat, E. L., D. J. J. van Hinsbergen, M. Maffione, C. G. Langereis, R. L. M. Vissers, A.  
695 Cherchi, R. Schroeder, H. Madani, and S. Columbu (2014), Eocene rotation of Sardinia,  
696 and the paleogeography of the western Mediterranean region, *Earth and Planetary  
697 Science Letters*, 401, 183-195, doi: 10.1016/j.epsl.2014.06.012.
- 698 Alberti, M., F.A. Decandia, and E. Tavarnelli (1998), Kinematic evolution of the outer zones  
699 of the Northern Apennines, Italy: the contribution of sequential cross-section -balancing  
700 techniques. *Mem. Soc. Geol. It.*, 52, 607-616.
- 701 Amante, C., and B. W. Eakins (2009), ETOPO1 1 Arc-Minute Global Relief Model:  
702 Procedures, Data Sources and Analysis, NOAA Technical Memorandum NESDIS  
703 NGDC-24, National Geophysical Data Center, NOAA.

704 Amaru, M. L. (2007), Global travel time tomography with 3-D reference models, *Geologica*  
705 *Ultraiectina*, 274.

706 Anderson, H., and J. Jackson (1987), Active tectonics of the Adriatic Region, *Geophysical*  
707 *Journal of the Royal Astronomical Society*, 91, 937-983.

708 Argnani, A. (1990), The strait of Sicily rift zone: foreland deformation related to the evolution  
709 of a back-arc basin, *Journal of Geodynamics*, 12, 311-331.

710 Argnani, A., and Ricci Lucchi F. (2001), Tertiary Siliciclastic Turbidite Systems. In: G.B. Vai  
711 and I.P. Martini (eds.), *Anatomy of a Mountain: the Apennines and adjacent*  
712 *Mediterranean basins*. Kluwer Academic Publisher, London, 327-350.

713 Babić, L., P. A. Hochuli, and J. Zupanic (2002), The Jurassic ophiolitic melange in the NE  
714 Dinarides: Dating, internal structure and geotectonic implications, *Eclogae Geologicae*  
715 *Helveticae*, 95(3), doi: 10.5169/seals-168959.

716 Bally, A.W., L. Burbi, C. Cooper, and R. Ghelardoni (1986), Balanced sections and seismic  
717 reflection profiles across the Central Apennines. *Mem. Soc. Geol. It.*, 35, 237-310.

718 Barchi, M. R., A. De Feyter, M. B. Magnani, G. Minelli, G. Pialli, and M. Sotera (1998a),  
719 Extensional tectonics in the Northern Apennines (Italy): Evidence from the CROP 03  
720 deep seismic reflection line, *Mem. Soc. Geol. It.*, 52, 527-538.

721 Barchi, M. R., A. De Feyter, M. B. Magnani, G. Minelli, G. Pialli, and B. M. Sotera (1998b),  
722 The structural style of the Umbria-Marche fold and thrust belt, *Mem. Soc. Geol. It.*, 52,  
723 557-578.

724 Barchi, M. R., G. Minelli, B. Magnani, and A. Mazzotti (2003), CROP 03: Northern  
725 Apennines, *Mem. Descr. Carta Geol. d'It.*, LXII, 127-136.

726 Bega, Z. (2013), Exploration opportunities in Albania – A Review of Recent Exploration  
727 Activities. Abstract, 7th Congress of the Balkan Geophysical Society, Tirana, Albania.

728 Bega, Z. (2015), Hydrocarbon exporation potential of Montenegro – a brief review, *Journal of*  
729 *Petroleum Geology*, 38(3), 317-330.

730 Benoit, M. H., M. Torpey, K. Liszewski (2011), P and S wave upper mantle seismic velocity  
731 structure beneath the northern Apennines: New evidence for the end of subduction,  
732 *Geochemistry, Geophysics, Geosystems G3*, 12(6), doi:10.1029/2010GC003428

733 Bennett, R. A., E. Serpelloni, E., S. Hreinsdóttir, M.T. Brandon, G. Buble, T. Basic, G.  
734 Casale, A. Cavaliere, M. Anzidei, M. Marjonovic, G. Minelli, G. Molli, and A.  
735 Montanari (2012), Syn-convergent extension observed using the RETREAT GPS  
736 network, northern Apennines, Italy. *J. Geophys. Res.*, 117, B04408, doi: 10.1029/  
737 2011JB008744.

738 Bianco, C., Brogi, A., Caggianelli, A., Giorgetti, G., Liotta, D., Meccheri, M. (2015), HP-LT  
739 metamorphism in the Elba Island: implications for the geodynamic evolution of the  
740 inner Northern Apennines (Italy), *Journal of Geodynamics*, 91, 13-25.

741 Biju-Duval, B., J. Dercourt, and X. Le Pichon (1977). From the Tethys ocean to the  
742 Mediterranean seas: a plate tectonic model of the evolution of the western Alpine  
743 system, *International symposium on the structural history of the Mediterranean basins*  
744 edited by B. Biju-Duval and L. Montadert, pp. 143-164.

745 Bird, P. (1979), Continental delamination and the Colorado Plateau, *Journal of Geophysical*  
746 *Research*, 84(B13), 7561-7571, doi: 10.1029/JB084iB13p07561.

747 Boyden, J. R., R. D. Müller, M. Gurnis, T. H. Torsvik, J. Clark, M. Turner, H. Ivey-Law, R.  
748 Watson, and J. Cannon (2011), Next-Generation plate-tectonic reconstructions using  
749 GPlates, in *Geoinformatics*, edited by R. Keller and C. Baru, pp. 95-114, Cambridge  
750 University Press.

751 Brogi, A., and D. Liotta, (2006), Understanding the crustal structures in Southern Tuscany:  
752 The contribution of CROP18. *Bollettino Geofisica Teorica Applicata*, 47(3), 401-423.

753 Butler, R.W.H., E. Tavarnelli, and M. Grasso (2006), Structural Inheritance in Mountain  
754 Belts: An Alpine-Apennine Perspective. *Journal of Structural Geology*, 28, 1893-1908.

- 755 Calais, E., J.-M. Nocquet, F. Jouanne, and M. Tardy (2002), Current strain regime in the  
756 Western Alps from continuous Global Positioning System measurements, 1996-2001,  
757 *Geology*, 20(7), 651-654.
- 758 Calamita, F., G. Cello, C. Invernizzi, and W. Paltrinieri (1990), Stile strutturale e cronologia  
759 della deformazione lungo la traversa M. S. Vicino-Polverigi (Appennino marchigiano  
760 esterno). *Atti Convegno: Neogene Thrust Tectonics*. Parma 8- 9 Giugno 1990. *Studi*  
761 *Geol. Camerti*, volume special.
- 762 Calamita, F., and G. Deiana (1988), The arcuate shape of the Umbria-Marche-Sabina  
763 Apennines (Central Italy). *Tectonophysics*, 146, 139-147.
- 764 Capitano, F. A., and S. Goes (2006), Mesozoic spreading kinematics: consequences for  
765 Cenozoic Central and Western Mediterranean subduction. *Geophysical Journal*  
766 *International*, 165(3), 804–816.
- 767 Carminati E., and C. Doglioni (2012), Alps vs. Apennines: The paradigm of a tectonically  
768 asymmetric Earth, *Earth-Science Reviews*, 112, 67–96.
- 769 Catalano, R., C. Doglioni, and S. Merlini (2001), On the Mesozoic Ionian Basin, *Geophys. J.*  
770 *Int.*, 144, 49–64, doi:10.1046/j.0956-540X.2000.01287.x.
- 771 Cerrina Feroni, A., L. Martell, P. Martinelli, G. Ottria, and R. Catanzariti (2002). *Carta*  
772 *Geologico-Strutturale dell’Appennino Emiliano-Romagnolo-Note Illustrative*. Regione  
773 Emilia-Romagna. Selca Firenze.
- 774 Channell, J. E. T. (1996), Palaeomagnetism and palaeogeography of Adria, In: Morris, A.,  
775 Tarling, D.H. (Eds.), *Palaeomagnetism and Tectonics of the Mediterranean Region*.  
776 Geological Society, London, Special Publications, pp. 119– 132.
- 777 Channell, J. E. T., B. D’Argenio, and F. Horvath (1979), Adria, the African Promontory, in  
778 *Mesozoic Mediterranean Palaeogeography*, *Earth Science Reviews*, 15, 213-292.
- 779 Channell, J. E. T., and F. Horváth (1976), The African/Adriatic promontory as a  
780 palaeogeographical premise for alpine orogeny and plate movements in the Carpatho-  
781 Balkan region, *Tectonophysics*, 35(1-3), 71-101, doi: 10.1016/0040-1951(76)90030-5.
- 782 Channell, J. E. T., and J. C. Mareschal (1989), Delamination and asymmetric lithospheric  
783 thickening in the development of the Tyrrhenian Rift, *Geol. Soc., London, Spec. Publ.*,  
784 45(1), 285-302.
- 785 Chiarabba, C., P. De Gori, and F. Speranza (2009), Deep geometry and rheology of an  
786 orogenic wedge developing above a continental subduction zone: Seismological  
787 evidence from the northern-central Apennines (Italy), *Lithosphere*, 1(2), 95-104.
- 788 Chiarabba, C., G. Giacomuzzi I. Bianchi, N. P. Agostinetti, J. Park (2014), From underplating  
789 to delamination-retreat in the northern Apennines, *Earth and Planetary Science Letters*,  
790 403, 108-116.
- 791 Civile, D., E. Lodolo, D. Accettella, R. Geletti, Z. Ben-Avraham, M. Deponte, L. Facchin, R.  
792 Ramella, and R. Romeo (2010), The Pantelleria graben (Sicily Channel, Central  
793 Mediterranean): An example of intraplate ‘passive’ rift, *Tectonophysics*, 490, 173-183.
- 794 Civile, D., E. Lodolo, L. Tortorici, G. Lamza fame, and G. Brancolini (2008), Relationships  
795 between magmatism and tectonics in a continental rift: The Pantelleria Island region  
796 (Sicily Channel, Italy), *Marine Geology*, 251, 32-46, doi:  
797 10.1016/j.margeo.2008.01.009.
- 798 Collombet, M., J. C. Thomas, A. Chauvin, P. Tricart, J. P. Bouillin, and J. P. Gratier (2002),  
799 Counterclockwise rotation of the western Alps since the Oligocene: New insights from  
800 paleomagnetic data, *Tectonics*, 21(4), doi: 10.1029/2001TC901016.
- 801 Cornamusini, G. (2004), Sand-rich turbidite system of the Late Oligocene Northern  
802 Apennines foredeep: physical stratigraphy and architecture of the ‘Macigno costiero’  
803 (coastal Tuscany, Italy), *Geol. Pub., London, Special Publications*, 222, 261-283.
- 804 Cornamusini G., A. Lazzarotto, S. Merlini, and V. Pascucci (2002), Eocene-Miocene  
805 evolution of the north Tyrrhenian Sea, *Boll. Soc. Geol. Ital., Spec.1*, 769-787.

806 Corti, G., M. Cuffaro, C. Doglioni, F. Innocenti, and P. Manetti (2006), Coexisting  
807 geodynamic processes in the Sicily Channel, in: Dilek, Y. and Pavlides, S., eds.,  
808 Postcollisional tectonics and magmatism in the Mediterranean region and Asia:  
809 Geological Society of America Special Paper 409, 83-96, doi: 10.113/2006.2409(05).

810 Coward, M.P., M. De Donatis, S. Mazzoli, W. Paltrinieri, and F.C. Wezel (1999), Frontal part  
811 of the northern Apennines fold and thrust belt in the Romagna-Marche area (Italy):  
812 shallow and deep structural styles, *Tectonics*, 18, 559-574.

813 Cowie, L., and N. Kuznir (2012), Mapping crustal thickness and oceanic lithosphere  
814 distribution in the Eastern Mediterranean using gravity inversion, *Petroleum*  
815 *Geoscience*, 18, 373-380.

816 D'Agostino, N., A. Avallone, D. Cheloni, E. D'Anastasio, S. Mantenuto and G. Selvaggi  
817 (2008), Active tectonics of the Adriatic region from GPS and earthquake slip vectors,  
818 *Journal of Geophysical Research*, 113, B12413, doi: 10.1029/2008.JB005860.

819 Decandia F.A., A. Lazzarotto, D. Liotta, L. Cernobori, and R. Nicolich (1998), The CROP03  
820 traverse: insights on postcollisional evolution of Northern Apennines. *Mem. Soc. Geol.*  
821 *It.*, 52, 427-439.

822 Dercourt, J., Zonenshain, L.P., Ricou, L.-E., Kazmin, V.G., Le Pichon, X., Knipper, A.L.,  
823 Grandjaquet, C., Sbertshikov, I.M., Geyssant, J., Lepvrier, C., Pechersky, D.H., Boulin,  
824 J., Sibuet, J.-C., Savostin, L.A., Sorokhtin, O., Westphal, M., Bazhenov, M.L., Lauer,  
825 J.P. Bijou-Duval, B. (1986) Geological evolution of the Tethys belt from the Atlantic to  
826 the Pamirs since the Lias, *Tectonophysics*, 123, 241–315.

827 de Voogd, B., C. Truffert, N. Chamot-Rooke, P. Huchon, S. Lallemand, and X. Le Pichon  
828 (1992), Two-ship deep seismic soundings in the basins of the eastern Mediterranean Sea  
829 (Pasiphae cruise), *Geophys. J. Int.*, 109, 536–552, doi:10.1111/j.1365-  
830 246X.1992.tb00116.x.

831 Dewey, J. F., M. L. Helman, S. D. Knott, E. Turco, and D. H. W. Hutton (1989), Kinematics  
832 of the western Mediterranean, Geological Society, London, Special Publications, 45(1),  
833 265-283, doi: 10.1144/gsl.sp.1989.045.01.15.

834 Doglioni, C., and A. Bosellini, (1987), Eoalpine and Mesoalpine tectonics in the Southern  
835 Alps, *Geologische Rundschau*, 76, 735–754.

836 Doglioni, C., F. Innocenti, and G. Mariotti (2001), Why Mt Etna?, *Terra Nova*, 13(1), 25–31,  
837 doi:10.1046/j.1365-3121.2001.00301.x.

838 Doubrovine, P., and J. A. Tarduno (2008), Linking the Late Cretaceous to Paleogene Pacific  
839 plate and the Atlantic bordering continents using plate circuits and paleomagnetic data,  
840 *Journal of Geophysical Research*, 113, B07104, doi:10.1029/2008JB005584.

841 Faccenna, C., T. W. Becker, F. P. Lucente, L. Jolivet, and F. Rossetti (2001), History of  
842 subduction and back-arc extension in the Central Mediterranean, *Geophysical Journal*  
843 *International*, 145, 809-820.

844 Faccenna, C., L. Jolivet, C. Piromallo, and A. Morelli (2003), Subduction and the depth of  
845 convection in the Mediterranean mantle, *Journal of Geophysical Research*, 108(B2),  
846 doi: 10.1029/2001jb001690.

847 Faccenna, C., C. Piromallo, A. Crespo-Blanc, L. Jolivet, and F. Rossetti (2004), Lateral slab  
848 deformation and the origin of the western Mediterranean arcs, *Tectonics*, 23(1),  
849 TC1012, doi: 10.1029/2002tc001488.

850 Fantoni, R., R. Bersezio, and F. Forcella, (2004), Alpine structure and deformation  
851 chronology at the southern Alps-Po Plain border in Lombardy: *Bollettino della Societa*  
852 *Geologica Italiana*, 123, 463–476.

853 Favaro, S., M. R. Handy, A. Scharf, and R. Schuster (2017), Changing patterns of exhumation  
854 and denudation in front of an advancing crustal indenter, Tauern Window (Eastern  
855 Alps), *Tectonics*, 36, 10.1002/2016TC004448.

856 Frisch, W. (1979), Tectonic progradation and plate tectonic evolution of the Alps.



857 Tectonophysics 60, 121–139.

858 Frizon de Lamotte, D., C. Raulin, N. Mouchot, J.-C. Wrobel-Daveau, C. Blanpied, and J.-C.  
859 Ringenbach (2011), The southernmost margin of the Tethys realm during the Mesozoic  
860 and Cenozoic: Initial geometry and timing of the inversion processes, *Tectonics*, 30,  
861 TC3002, doi:10.1029/2010TC002691.

862 Fügenschuh, B., and S. M. Schmid (2005), Age and significance of core complex formation in  
863 a very curved orogen: evidence from fission track studies in the South Carpathians  
864 (Romania). *Tectonophysics* 404, 33–53.

865 Gaina, C., T. H. Torsvik, D. J. J. van Hinsbergen, S. Medvedev, S. C. Werner, and C. Labails  
866 (2013), The African Plate: A history of oceanic crust accretion and subduction since the  
867 Jurassic, *Tectonophysics*, 604, 4–25, doi: 10.1016/j.tecto.2013.05.037.

868 Gallais, F., M. A. Gutscher, D. Graindorge, N. Chamot-Rooke, and D. Klaeschen (2011), A  
869 Miocene tectonic inversion in the Ionian Sea (central Mediterranean): Evidence from  
870 multi-channel seismic data, *Journal of Geophysical Research*, 116, B12108, doi:  
871 10.1029/2011JB008505.

872 Gattacceca, J., A. Deino, R. Rizzo, D. S. Jones, B. Henry, B. Beaudoin, and F. Vadeboin  
873 (2007), Miocene rotation of Sardinia: New paleomagnetic and geochronological  
874 constraints and geodynamic implications, *Earth and Planetary Science Letters*, 258(3-4),  
875 359–377, doi: 10.1016/j.epsl.2007.02.003.

876 Gueguen, E., C. Doglioni, and M. Fernandez (1997), On the post-25 Ma geodynamic  
877 evolution of the western Mediterranean, *Tectonophysics*, 298, 259–269.

878 Gutscher, M. A., S. Dominguez, B. M. de Lapinai, L. Pinheiro, F. Gallais, N. Babonneau, A.  
879 Cattaneo, Y. Le Faou, G. Barreca, A. Micallef and M. Rovere (2016), Tectonic  
880 expression of an active slab tear from high-resolution seismic and bathymetric data  
881 offshore Sicily (Ionian Sea), *Tectonics*, doi: 10.1002/2015TC003898.

882 Hall, R., and W. Spakman (2015), Mantle structure and tectonic history of SE Asia,  
883 *Tectonophysics* 658, 14–5.

884 Handy, M. R., B. Fügenschuh, J. Giese, E. Le Breton, B. Muceku, K. Onuzi, J. Pleuger, S. M.  
885 Schmid, and K. Ustaszewski (2015a), Orogen-parallel and -normal extension at the  
886 Dinarides-Hellenides junction during clockwise rotation and radial expansion of the  
887 retreating Hellenic arc-trench system. AGU 2015-T23F-06, American Geophysical  
888 Union Fall Meeting, San Francisco, U.S.A.

889 Handy, M. R., S. M. Schmid, R. Bousquet, E. Kissling, and D. Bernoulli (2010), Reconciling  
890 plate-tectonic reconstructions of Alpine Tethys with the geological–geophysical record  
891 of spreading and subduction in the Alps, *Earth-Science Reviews*, 102(3-4), 121–158,  
892 doi: 10.1016/j.earscirev.2010.06.002.

893 Handy, M. R., S. M. Schmid, S. Cionoiu, C. Deutsch, S. Evseev, J. Giese, S. Groß, E. Le  
894 Breton, K. Onuzi, J. Pleuger, K. Ustaszewski, D. Wannek, and S. Zertani (2014),  
895 Tectonics related to rotation at the western end of the Skutari-Pec Normal Fault.  
896 Abstract volume, 1, 126–127. 20<sup>th</sup> Meeting of the Carpatho-Balkan Geological  
897 Association (CBGA), 23–25.09.2014 in Tirana, Albania.

898 Handy, M. R., K. Ustaszewski, and E. Kissling (2015b), Reconstructing the Alps–  
899 Carpathians–Dinarides as a key to understanding switches in subduction polarity, slab  
900 gaps and surface motion, *International Journal of Earth Sciences*, 104(1), 1–26, doi:  
901 10.1007/s00531-014-1060-3.

902 Handy M. R., and A. Zingg (1991), The tectonic and rheologic evolution of an attenuated  
903 cross section of the continental crust: Ivrea crustal section, southern Alps, northwestern  
904 Italy and southern Switzerland. *Geol Soc Am Bull*, 103:236–253.

905 Hieke, W., H. B. Hirschleber, and G. A. Dehmani (2003), The Ionian Abyssal Plain (central  
906 Mediterranean Sea): Morphology, subbottom structures and geodynamic history – an

907 inventory, *Marine Geophysical Researches*, 24, 279-310, doi: 10.1007/s11001-004-  
908 2173-z.

909 Jolivet, L., and C. Faccenna (2000), Mediterranean extension and the Africa–Eurasia  
910 collision. *Tectonics*, 19, 1095–1106.

911 Jolivet, L., C. Faccenna, B. Goffé, M. Mattei, F. Rossetti, C. Brunet, F. Storti, R. Funiviello,  
912 J.-P. Cadet, N. d’Agostino, and T. Parrra, (1998), Midcrustal shear zones in  
913 postorogenic extension: example from the northern Tyrrhenian Sea, *J. geophys.Res.*,  
914 103 (B6), 12 123–12 161, doi: 10.1029/97JB03616.

915 Jolivet, L., C. Gorini, J. Smit, and S. Leroy (2015), Continental breakup and the dynamics of  
916 rifting in back-arc basins: The Gulf of Lion margin, *Tectonics*, 34(4), 662-679, doi:  
917 10.1002/2014tc003570.

918 Jongsma, D., J. M. Woodside, G. C. P. King, and J. E. van Hinte (1987), The Medina  
919 Wrench: a key to the kinematics of the central and eastern Mediterranean over the past 5  
920 Ma, *Earth and Planetary Science Letters*, 83, 87-106.

921 Kastelić, V., M. Vrabec, D. Cunningham, and A. Gosar (2008), Neo-Alpine structural  
922 evolution and present-day tectonic activity of the eastern Southern Alps: The case of the  
923 Ravne Fault, NW Slovenia. *Journal of Structural Geology*, 30, 963-975. Kirkwood,  
924 B.H., Royer, J.-Y., Chang, T.C., Gordon, R.G., 1999. Statistical tools for estimating and  
925 combining finite rotations and their uncertainties, *Geophysical Journal International*,  
926 137(2), 408-428.

927 Kissel, C., and F. Speranza (1995), Paleomagnetism of external southern and central  
928 Dinarides and northern Albanides: Implications for the Cenozoic activity of the Scutari-  
929 Pec transverse zone, *Journal of Geophysical Research*, 100(B8), 14,999-1,5000.

930 Lacassin, R. (1987), Kinematics of ductile shearing from outcrop to crustal scale in the Monte  
931 Rosa nappe, Western Alps, *Tectonics*, 6(1), 69-88.

932 Lavecchia, G., G. Minelli, and G. Pialli (1987), Contractional and extensional tectonics along  
933 the transect Trasimeno Lake - Pesaro (Central Italy). In "The lithosphere in Italy:  
934 advances in earth sciences research" - Accademia dei Lincei, Roma, 143-165.

935 Le Pichon, X., J. C. Sibuet, and J. Francheteau (1977), The fit of continents around the North  
936 Atlantic Ocean, *Tectonophysics*, 38, 169-209.

937 Linzer, H.-G., K. Decker, H. Peresson, R. Dell’Mour, and W. Frisch (2002), Balancing lateral  
938 orogenic float of the Eastern Alps. *Tectonophysics*, 354, 211-237, doi: 10.1016/S0040-  
939 1951(02)00337-2.

940 Lippitsch, R., Kissling, E., Ansorge, J., 2003. Upper mantle structure beneath the Alpine  
941 orogene from high-resolution teleseismic tomography. *Journal of Geophysical  
942 Research*, 108, doi: 10.1029/2002JB002016

943 Malinverno, A., and W. B. F. Ryan (1986), Extension in the Tyrrhenian Sea and shortening in  
944 the Apennines as result of arc migration driven by sinking of the lithosphere, *Tectonics*,  
945 5(2), 227-245, doi: 10.1029/TC005i002p00227.

946 Martin, L. A. J., D. Rubatto, A. V. Brovarone, and J. Hermann (2011), Late Eocene  
947 lawsonite-eclogite facies metasomatism of a granulite silver associated to ophiolites in  
948 Alpine Corsica, *Lithos*, 125, 620-640, doi: 10.1016/j.lithos.2011.03.015.

949 Márton, E. (2003), Palaeomagnetic evidence for Tertiary counterclockwise rotation of Adria,  
950 *Tectonophysics*, 377(1-2), 143-156, doi: 10.1016/j.tecto.2003.08.022.

951 Márton, E., V. Čosović, A. Moro, and S. Zvocak (2008), The motion of Adria during the Late  
952 Jurassic and Cretaceous: New paleomagnetic results from stable Istria, *Tectonophysics*,  
953 454(1-4), 44-53, doi: 10.1016/j.tecto.2008.04.002.

954 Márton, E., D. Zampieri, P. Grandesso, V. Čosović, and A. Moro (2010), New Cretaceous  
955 paleomagnetic results from the foreland of the Southern Alps and the refined apparent  
956 polar wander path for stable Adria, *Tectonophysics*, 480(1-4), 57-72, doi:  
957 10.1016/j.tecto.2009.09.003.

958 Márton, E., D. Zampieri, M. Kázmér, I. Dunkl, and W. Frisch (2011), New Paleocene–Eocene  
959 paleomagnetic results from the foreland of the Southern Alps confirm decoupling of  
960 stable Adria from the African plate, *Tectonophysics*, 504(1-4), 89-99, doi:  
961 10.1016/j.tecto.2011.03.006.

962 Matenco, L., and Radivojević, D., 2012. On the formation and evolution of the Pannonian  
963 Basin: constraints derived from the orogenic collapse recorded at the junction between  
964 the Carpathians and Dinarides. *Tectonics*, v. 31, doi:10.1029/2012TC003206. issn:  
965 0278-7407.

966 Mauffret, A., D. Frizon de Lamotte, S. Lallemand, C. Gorini and A. Maillard (2004), E-W  
967 opening of the Algerian Basin (Western Mediterranean), *Terra Nova*, 16(5), 257-264,  
968 doi: 10.1111/j.1365-3121.2004.00559.x.

969 Mazzoli, S., and M. Helman (1994), Neogene patterns of relative motion for Africa-Europe:  
970 some implications for recent central Mediterranean tectonics. *International Journal of*  
971 *Earth Science*, 83, 464-468.

972 Mazzoli, S., P. P. Pierantoni, F. Borraccini, W. Paltrinier, and G. Deiana, (2005), Geometry,  
973 segmentation pattern and displacement variations along a major Apennine thrust zone,  
974 central Italy, *Journal of Structural Geology*, 27, 1940–1953

975 Mele, G. (2001), The Adriatic lithosphere is a promontory of the African Plate: Evidence of a  
976 continuous mantle lid in the Ionian Sea from efficient Sn propagation, *Geophysical*  
977 *Research Letters*, 28(3), doi: 10.1029/2000GL012148.

978 Molli, G. (2008), Northern Apennine-Corsica orogenic system: an updated overview,  
979 *Geological Society, London, Special Publications*, 298(1), 413-442, doi:  
980 10.1144/sp298.19.

981 Molli, G., G. Giorgetti, and M. Meccheri (2000), Structural and petrological constraints on the  
982 tectono-metamorphic evolution of the Massa Unit (Alpi Apuane, NW Tuscany, Italy),  
983 *Geological Journal*, 35(3-4), 251-264, doi: 10.1002/gj.860.

984 Molli, G., and J. Malavieille (2011), Orogenic processes and the Corsica/Apennines  
985 geodynamic evolution: insights from Taiwan, *International Journal of Earth Sciences*,  
986 100(5), 1207-1224, doi:10.1007/s00531-010-0598-y.

987 Moretti, I., and L. Royden (1988), Deflection, gravity anomalies and tectonics of doubly  
988 subducted continental lithosphere: Adriatic and Ionian Seas, *Tectonics*, 7(4), 875-893.

989 Morgan, W. J. (1968), Rises, trenches, great faults, and crustal blocks, *Journal of Geophysical*  
990 *Research*, 73, 1959–82.

991 Munzarová, H., J. Plomerová, V. Babuška, and L. Vecsey (2013), Upper-mantle fabrics  
992 beneath the Northern Apennines revealed by seismic anisotropy, *Geochemistry,*  
993 *Geophysics, Geosystems*, 14(4), 1156-1181, doi: 10.1002/ggge.20092.

994 Muttoni, G., E. Dallanave, and J. E. T. Channell, (2013), The drift history of Adria and Africa  
995 from 280 Ma to Present, Jurassic true polar wander, and zonal climate control on  
996 Tethyan sedimentary facies, *Palaeogeography, Palaeoclimatology, Palaeoecology*, 386,  
997 415-435.

998 Oldow, J., L. Ferranti, D. S. Lewis, J. K. Campbell, B. D'Argenio, R. Catalano, G. Pappone,  
999 L. Carmignani, P. Conti, and C. L. V. Aiken (2002), Active fragmentation of Adria, the  
1000 north African promontory, central Mediterranean orogen, *Geology*, 30(9), 779–782.

1001 Pamić, J., I. Gušić, and V. Jelaska (1998), Geodynamic evolution of the Central Dinarides,  
1002 *Tectonophysics*, 297, 251-268.

1003 Patacca, E., R. Sartori, and P. Scandone (1990), Tyrrhenian basin and Apenninic arcs:  
1004 kinematic relations since Late-Tortonian times, *Mem. Soc. Geol. It*, 45, 425-451.

1005 Picha, F. J. (2002), Late orogenic strike-slip faulting and escape tectonics in the frontal  
1006 Dinarides-Hellenides, Croatia, Yugoslavia, Albania, and Greece, *AAPG Bulletin* 86,  
1007 1659–1671.

- 1008 Piromallo, C., and A. Morelli (2003), P-wave tomography of the mantle under the Alpine-  
1009 Mediterranean area, *Journal of Geophysical Research*, 108(B2), doi:  
1010 10.1029/2002jb001757.
- 1011 Polonia, A., L. Torelli, P. Mussoni, L. Gasperini, A. Artoni, and D. Klaeschen (2011), The  
1012 Calabrian Arc subduction complex in the Ionian Sea: Regional architecture, active  
1013 deformation, and seismic hazard, *Tectonics*, 30, TC5018, doi: 10.1029/2011TC002821.
- 1014 Ricou, L. E. (1994), Tethys reconstructed: Plates continental fragments and their boundaries  
1015 since 260 Ma from Central America to south-eastern Asia, *Geodinamica Acta*, 7, 169-  
1016 218.
- 1017 Rosenbaum, G., G. S. Lister, and C. Doubos (2004), Mesozoic and Cenozoic motion of Adria  
1018 (central Mediterranean): a review of constraints and limitations, *Geodinamica Acta*,  
1019 17(2), 125-139.
- 1020 Roure, F., P. Casero, and B. Addoum (2012), Alpine inversion of the North African margin  
1021 and delamination of its continental lithosphere, *Tectonics*, 31, TC3006, doi:  
1022 10.1029/2011TC002989.
- 1023 Roure, F., S. Nazaj, K. Mushka, I. Fili, J. P. Cadet, and M. Bonneau (2004), Kinematic  
1024 evolution and petroleum systems: an appraisal of the Outer Albanides, Thrust tectonics  
1025 and hydrocarbon systems, 82, 474-493.
- 1026 Royden, L.H. (1993), The tectonic expression of slab pull at continental convergent  
1027 boundaries, *Tectonics*, 12(2), 303-325.
- 1028 Royden L. H., and B. C. Burchfiel (1989), Are systematic variations in thrust belt style related  
1029 to plate boundary processes? (The Western Alps versus the Carpathians), *Tectonics*,  
1030 8(1), 51-61.
- 1031 Royden, L., E. Patacca and P. Scandone (1987), Segmentation and configuration of subducted  
1032 lithosphere in Italy: an important control on thrust-belt and foredeep-basin evolution.  
1033 *Geology*, 15, 714–717.
- 1034 Sani F., G. Vannucci, M. Boccaletti, M. Bonini, G. Corti, and E. Serpelloni (2016), Insights  
1035 into the fragmentation of the Adria Plate, *Journal of Geodynamics*, 102, 121-138, doi:  
1036 10.1016/j.jog.2016.09.004, 121-138.
- 1037 Scharf, A., M. R. Handy, S. Favaro, S.M. Schmid, A. Bertrand (2013), Modes of orogen-  
1038 parallel stretching and extensional exhumation in response to microplate indentation and  
1039 roll-back subduction (Tauern Window, Eastern Alps), *International Journal of Earth  
1040 Sciences*, 102(6), 1627-1654, doi: 10.1007/s00531-013-0894-4.
- 1041 Schefer, S., V. Cvetković, B. Fügenschuh, A. Kounov, M. Ovtcharova, U. Schaltegger, S. M.  
1042 Schmid (2011), Triassic metasediments in the internal Dinarides (Kopaonik area,  
1043 southern Serbia): stratigraphy, paleogeographic and tectonic significance, *Geologica  
1044 Carpathica*, 61(2), doi: 10.2478/v10096-010-0003-6.
- 1045 Schmid, S. M., D. Bernoulli, B. Fügenschuh, L. Matenco, S. Schefer, S., R. Schuster, M.  
1046 Tischler, and K. Ustaszewski (2008), The Alpine–Carpathian–Dinaridic orogenic  
1047 system: correlation and evolution of tectonic units, *Swiss Journal of Geosciences*,  
1048 101(1), 139–183.
- 1049 Schmid, S. M., B. Fügenschuh, E. Kissling, and R. Schuster, R. (2004), Tectonic Map and  
1050 overall architecture of the Alpine orogeny, *Eclogae Geologicae Helvetiae*, 97 (1), 93–  
1051 117.
- 1052 Schmid, S. M., M. R. Handy, B. Fügenschuh, L. C. Matenco, B. Muceku, K. Onuzi, J.  
1053 Pleuger J., and K. Ustaszewski (2014), Nature and role of the Skutari-Pec Line in the  
1054 context of the geology of the Balkan Peninsula, Abstract volume, 1, 134, 20<sup>th</sup> Meeting  
1055 of the Carpatho-Balkan Geological Association (CBGA), Tirana, Albania.
- 1056 Schmid, S. M., E. Kissling, T. Diehl, D. J. J. van Hinsbergen, and G. Molli, (2017), Ivrea  
1057 mantle wedge, arc of the Western Alps, and kinematic evolution of the Alps–Apennines  
1058 orogenic system, *Swiss Journal of Geosciences*, doi: 10.1007/s00015-016-0237-0.

- 1059 Schmid, S. M., O. A. Pfiffner, N. Froitzheim, G. Schönborn, E. Kissling (1996),  
 1060 Geophysical–geological transect and tectonic evolution of the Swiss–Italian Alps,  
 1061 *Tectonics* 15 (5), 1036–1064.
- 1062 Schönborn, G. (1992). Alpine tectonics and kinematic models of the central Southern Alps.  
 1063 PhD Thesis.
- 1064 Schönborn, G. (1999). Balancing cross sections with kinematic constraints: The Dolomites  
 1065 (northern Italy), *Tectonics*, 18(3), 527-545
- 1066 Scisciani, V., and F. Calamita (2009), Active intraplate deformation within Adria: Examples  
 1067 from the Adriatic region, *Tectonophysics*, 476, 57–72.
- 1068 Seranne, M. (1999), The Gulf of Lion continental margin (NW Mediterranean) revisited by  
 1069 IBS: an overview, *Geological Society, London, Special Publications*, 156(1), 15-36,  
 1070 doi: 10.1144/gsl.sp.1999.156.01.03.
- 1071 Serri, G., F. Innocenti, and P. Manetti (1993), Geochemical and petrological evidence of the  
 1072 subduction of delaminated Adriatic continental lithosphere in the genesis of the  
 1073 Neogene-Quaternary magmatism of central Italy. *Tectonophysics*, 223, 117–147.
- 1074 Seton, M., Müller, R. D., Zahirovic, S., Gaina, C., Torsvik, T.H., Shephard, G., Talsma, A.,  
 1075 Gurnis, M., Turner, M., Maus, S., Chandler, M. (2012), Global continental and ocean  
 1076 basin reconstructions since 200Ma, *Earth-Science Reviews*, 113(3-4), 212-270, doi:  
 1077 10.1016/j.earscirev.2012.03.002.
- 1078 Spada, M., I. Bianchi, E. Kissling, N. P. Agostinetti, and S. Wiemer (2013), Combining  
 1079 controlled-source seismology and receiver function information to derive 3-D Moho  
 1080 topography for Italy, *Geophysical Journal International*, 194(2), 1050-1068, doi:  
 1081 10.1093/gji/ggt148.
- 1082 Speranza, F., L. Minelli, A. Pignatelli, and M. Chiappini (2012), The Ionian Sea: The oldest  
 1083 in situ ocean fragment of the world?, *Journal of Geophysical Research*, 117(B12), doi:  
 1084 10.1029/2012JB009475.
- 1085 Speranza, F, I. M. Villa, L. Sagnotti, F. Florindo, D. Cosentino, P. Cipollari, and M. Mattei  
 1086 (2002), Age of the Corsica-Sardinia rotation and Liguro-Provençal Basin spreading:  
 1087 new paleomagnetic and Ar/Ar evidence, *Tectonophysics*, 347, 231-251.
- 1088 Stampfli, G. M., and G. D. Borel (2002), A plate tectonic model for the Paleozoic and  
 1089 Mesozoic constrained by dynamic plate boundaries and restored synthetic oceanic  
 1090 isochrons, *Earth and Planetary Science Letters*, 196, 17-33.
- 1091 Stampfli, G. M., J. Mosar, S. Marquer, R. Marchant, T. Baudin, and G. Borel (1998),  
 1092 Subduction and obduction processes in the Swiss Alps *Tectonophysics*, 296, 159–204.
- 1093 Tari, V. (2002), Evolution of the northern and western Dinarides: a tectonostratigraphic  
 1094 approach, in *European Geosciences Union 2002*, edited, pp. 223-236, EGU Stephan  
 1095 Mueller Special Publication Series.
- 1096 Tavarnelli E., R. W. H. Butler, F. A. Decandia, F. Calamita, M. Grasso, W. Alvarez, and P.  
 1097 Renda (2004), Implications of fault reactivation and structural inheritance in the  
 1098 Cenozoic tectonic evolution of Italy. In: Crescenti U., D'Offizi S., Merlini S. & Sacchi  
 1099 R. (eds.) "Geology of Italy" - Special Volume of the Società Geologica Italiana for the  
 1100 32<sup>nd</sup> International Geological Congress (IGC 32), Florence 2004, 209-222.
- 1101 Tavarnelli E., F.A. Decandia, P. Renda, M. Tramutoli, E. Gueguen, and M. Alberti (2001),  
 1102 Repeated reactivation in the Apennine-Maghrebide system, Italy: a possible example of  
 1103 fault-zone weakening? *Geological Society of London Special Publication* 186, "The  
 1104 Nature and Tectonic Significance of Fault Zone Weakening" (Holdsworth, R.E.,  
 1105 Strachan, R.A., Magloughlin, J.F. & Knipe, R.J., Eds.), 273-286.
- 1106 Theye, T., J. Reinhardt, B. Goffé, L. Jolivet, and C. Brunet (1997), Ferro- and  
 1107 magnesiocarpholite from the Monte Argentario (Italy): First evidence for high-pressure  
 1108 metamorphism of the metasedimentary Verrucano sequence, and significance for P-T  
 1109 path reconstruction, *European Journal of Mineralogy*, 9(4), 859-874, doi:

1110 10.1127/ejm/9/4/0859.

1111 Ustaszewski, K., A. Kounov, S. M. Schmid, U. Schaltegger, E. Krenn, W. Frank, and B.

1112 Fügenschuh (2010), Evolution of the Adria-Europe plate boundary in the northern

1113 Dinarides: From continent-continent collision to back-arc extension, *Tectonics*, 29(6),

1114 doi: 10.1029/2010tc002668.

1115 Ustaszewski, K., S. M. Schmid, B. Fügenschuh, M. Tischler, E. Kissling, and W. Spakman

1116 (2008), A map-view restoration of the Alpine-Carpathian-Dinaridic system for the Early

1117 Miocene, *Swiss Journal of Geosciences*, 101(S1), 273-294, doi: 10.1007/s00015-008-

1118 1288-7.

1119 van Hinsbergen, D. J. J., E. Hafkenscheid, W. Spakman, J. E. Meulenkaamp, and M. J. R.

1120 Wortel (2005), Nappe stacking resulting from subduction of oceanic and continental

1121 lithosphere below Greece, *Geology*, 33(4), 325-328.

1122 van Hinsbergen, D. J. J., M. Mensink, C. G. Langereis, M. Maffione, L. Spalluto, M.

1123 Tropeano, and L. Sabato (2014a), Did Adria rotate relative to Africa?, *Solid Earth*, 5(2),

1124 611-629, doi: 10.5194/se-5-611-2014.

1125 van Hinsbergen, D. J. J., and S. M. Schmid (2012), Map view restoration of Aegean-West

1126 Anatolian accretion and extension since the Eocene, *Tectonics*, 31, TC5005,

1127 doi:10.1029/2012TC003132.

1128 van Hinsbergen, D. J. J., R. L. M. Vissers, W. Spakman (2014b), Origin and consequences of

1129 western Mediterranean subduction, rollback, and slab segmentation, *Tectonics*, 33, 393-

1130 419, doi:10.1002/tect.20125.

1131 Vignaroli, G., C. Faccenna, L. Jolivet, C. Piromallo, and F. Rossetti (2008), Subduction

1132 polarity reversal at the junction between the Western Alps and the Northern Apennines,

1133 Italy, *Tectonophysics*, 450, 34-50.

1134 Vissers, R. L. M., D. J. J. van Hinsbergen, P. Th. Meijer, and G. B. Piccardo (2013),

1135 Kinematics of Jurassic ultra-slow spreading in the Piemonte Ligurian ocean, *Earth and*

1136 *Planetary Science Letters*, 380, 138-150.

1137 Viti, M., E. Mantovani, D. Babbucci, C. Tamburelli, N. Cenni (2016), Seismotectonic of

1138 Padanian belt and surrounding belts: Which driving mechanism?, *International Journal*

1139 *of Geosciences*, 7, 1412-1451.

1140 von Blanckenburg, F., and J. H. Davies (1995), Slab breakoff: a model for syncollisional

1141 magmatism and tectonics in the Alps., *Tectonics*, 14(1), 120-131, doi:

1142 10.1029/94TC02051.

1143 Vrabc, M., and L. Fodor (2006), Late Cenozoic tectonics of Slovenia: structural styles at the

1144 Northeastern corner of the Adriatic microplate. In the Adria microplate: GPS geodesy,

1145 tectonics and hazards (pp. 151-168), Springer Netherlands.

1146 Wortel, M. J. R., and W. Spakman (2000), Subduction and slab detachment in the

1147 Mediterranean-Carpathian region, *Science*, 290, 1910-1917, doi:

1148 10.1126/science.290.5498.1910.

1149 Zingg A, M. R. Handy, J. C. Hunziker, S. M. Schmid (1990), Tectonometamorphic history of

1150 the Ivrea zone and its relation to the crustal evolution of the Southern Alps,

1151 *Tectonophysics*, 182, 169-192.

1152

1153 **Table**

1154

	<i>Dataset used to determine amount of post-20 Ma Adria rotation</i>	<i>Rotation (R2) for Model 1: 113 km convergence in western Alps (R1)</i>	<i>Rotation (R2) for Model 2: 60 km convergence in western Alps (R1)</i>
<i>Liguro-Provençal Basin (A-A')</i>	40 km spreading	Maximum $7.75 \pm 11.75^\circ$ (from $4^\circ$ CW to $19.5^\circ$ CCW)	Maximum $7.25 \pm 11.75^\circ$ (from $4.5^\circ$ CW to $19^\circ$ CCW)
<i>Tyrrhenian Sea – Tuscany (A'-A'')</i>	107 $\pm$ 14 km extension assuming 40 km initial thickness 51 $\pm$ 18 km extension assuming 30 km initial thickness $\Rightarrow$ 33-121 km divergence		
<i>Northern Apennines (A'-A'')</i>	30-60 km shortening assuming thick-skinned 100 km assuming thin-skinned $\Rightarrow$ minimum 30-100 km convergence		
<i>Southern Dinarides – Carpatho-Balkan (B-B')</i>	20 km crustal shortening 140 km slab-length $\Rightarrow$ 20-140 km convergence	Minimum $0.6^\circ$ CCW Maximum $7^\circ$ CCW	Minimum $0.3^\circ$ CCW Maximum $8^\circ$ CCW
<i>Eastern Alps (C-C')</i>	115-150 km convergence	$6.5 \pm 3^\circ$ CCW	$14 \pm 3^\circ$ CCW
<i>SCRZ (D-D')</i>	Minimum 30 km divergence	Minimum $3.5^\circ$ CCW	Minimum $4^\circ$ CCW
<b><i>Best-fit rotation</i></b>		<b><math>5.25^\circ \pm 1.75^\circ</math> CCW</b>	<b>No possible fit!</b>

1155 **Table 1.** Compilation of crustal shortening, extension, and Adria-Europe divergence and  
1156 convergence along transects A-A'-A'', B-B', C-C' and D-D' (location on Fig. 1) used to  
1157 constrain post-20 Ma Adria rotation relative to Europe (R1 and R2 refers to Fig. 6). Note that  
1158 a viable fit of those data is only obtained for Model 1 (involving 113 km convergence in  
1159 western Alps). More details on calculation of rotations are given in Appendix 1.

1160

1161 **Figure Captions**

1162

1163 **Figure 1.** Tectonic map of western Mediterranean with main Cenozoic structures and  
1164 geological-geophysical transects in this study. Tectonic structures compiled from *Seranne*  
1165 [1999], *Handy et al.* [2010; 2015b], *Civile et al.* [2010], *Frizon de Lamotte et al.* [2011] and  
1166 *Polonia et al.* [2011]. Background topographic-bathymetric map from ETOPO1 model  
1167 [*Amante and Eakins, 2009*]. Dashed black line in the Ionian Sea is the 4000 m depth isobath  
1168 delimiting the abyssal plain to the south [*Gallais et al. 2011*]. Abbreviations: Ad - Adige  
1169 Embayment; Ap - Apulia; CS - Corsica-Sardinia; Ga - Gargano; IS - Ionian Sea; Ist - Istria;  
1170 LP - Liguro-Provençal Basin; MAR - Mid-Adriatic Ridge; ME - Malta Escarpment; PB -  
1171 Pannonian Basin; SCRZ – Sicily Channel Rift Zone; SPNF, Shkoder-Peja Normal Fault; TS -  
1172 Tyrrhenian Sea. Map projection is Transverse Mercator (central meridian 10°E, latitude of  
1173 origin 43°N).

1174

1175 **Figure 2.** Comparison of Adria locations at 20 Ma depending on whether it moved together  
1176 with Africa (light green) or independently thereof based on data from the Alps [red; *Handy et*  
1177 *al., 2010; 2015b*] relative to Europe (grey). Finite Euler rotation poles for Africa (dark green)  
1178 from *Gaina et al.* [2013] and Corsica-Sardinia (orange) from *Seton et al.* [2012]. Numbers  
1179 indicate post-20 Ma overall divergence (+) and convergence (-) in the models. Present-day  
1180 location of plates and coastline are shown in black. Map projection on Figure 1.

1181

1182 **Figure 3. a.** Transect A-A'-A'' with Moho depth from *Spada et al.* [2013],  
1183 topography/bathymetry from ETOPO1 model [*Amante and Eakins, 2009*] and width of  
1184 oceanic crust (55 km, 21-16 Ma) in Liguro-Provençal Basin from *Jolivet et al.* [2015].  
1185 Location of transect on Figure 1. **b.** Transect A-A'-A'' after areal balancing of the crust  
1186 shows total extension in Liguro-Provençal and Tyrrhenian Sea. Note that the crust under  
1187 southern France was restored back to normal thickness (30 km), whereas under Corsica and  
1188 Italy the crust was restored to an orogenic thickness of 40 km (see text).

1189

1190 **Figure 4.** Tectonic map of the western Mediterranean showing post-20 Ma extension along  
1191 transect A-A'-A'' in red (Fig. 3) and post-20 Ma shortening in the northern Apennines along  
1192 the CROP03 profile, parallel to transect A'-A'', in green (location on Fig. 1). Map projection  
1193 shown on Figure 1.

1194



1195 **Figure 5.** P-wave tomography [model UU-P07 from *Amaru, 2007* and *Hall and Spakman,*  
1196 2015] along transect B-B' through the southern Dinarides-Carpatho-Balkan (location in Figs.  
1197 1 and 6) showing a positive anomaly (blue) interpreted as subducted Adriatic lithosphere.  
1198 Abbreviation: LAB – Lithosphere Asthenosphere Boundary.

1199

1200 **Figure 6.** Steps for reconstructing post-20 Ma motion path of Adria (yellow) relative to  
1201 Europe: (1) translate Ivrea to the SE by 113 km (Model 1) or 60 km (Model 2); (2) test  
1202 different rotations of Adria (20° CCW to 4° CW) around an axis located at translated Ivrea;  
1203 (3) calculate convergence and divergence along transects A'-A'', B-B', C-C', D-D' and  
1204 compare with dataset (Table 1). The finite Euler rotation pole (calculated with GPlates) for  
1205 Adria motion is a combination of Adria translation (R1) and rotation (R2). Post-20 Ma motion  
1206 of the Corsica-Sardinia block (blue) from *Speranza et al.* [2002; in compilation of *Seton et al.,*  
1207 2002] and of Africa (green) from *Gaina et al.* [2013] are taken into account when calculating  
1208 deformation along transect A-A'-A'' (blue arrows) and D-D' (green arrows), respectively.

1209

1210 **Figure 7.** Tectonic map of the central Mediterranean region showing location of the Adria  
1211 microplate and main front thrusts today (black) and at 20 Ma (pink, favored Model 1) relative  
1212 to Europe. Blue indicates the proposed force vectors driving the motion of Adria (push of  
1213 Africa from the south, pull of the Adriatic-Hellenic slab to the northeast) during crustal  
1214 wedging in the Alps that slowed and ultimately stopped Adria NW motion. Note the Neogene  
1215 NE-SW directed extension along the African margin that has accommodated divergence of  
1216 Adria and Africa. Abbreviations: CS - Corsica-Sardinia; LP - Liguro-Provençal; ME - Malta  
1217 Escarpment; PR - Pantelleria Rift; TS - Tyrrhenian Sea. Map projection on Figure 1.

1218

1219

1220

1221

1222

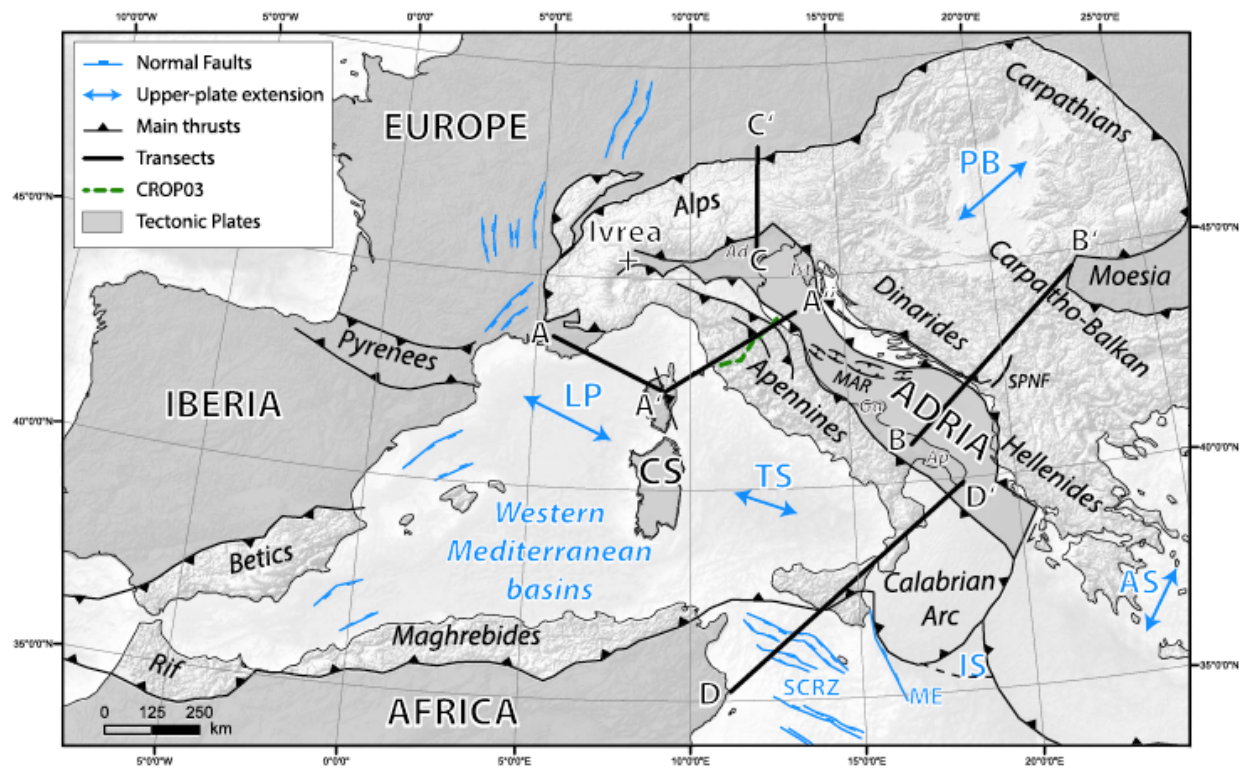


**FIGURE 1:** Tectonic map of western Mediterranean with main Cenozoic structures and geological-geophysical transects in this study. Tectonic structures compiled from Seranne (1999), Handy et al. (2010), Handy, Ustaszewski, et al. (2015), Civile et al. (2010), Frizon de Lamotte et al. (2011), and Polonia et al. (2011). Background topographic-bathymetric map from ETOPO1 model (Amante & Eakins, 2009). Dashed black line in the Ionian Sea is the 4,000 m depth isobath delimiting the abyssal plain to the south (Gallais et al., 2011). Abbreviations: Ad: Adige Embayment; Ap: Apulia; CS: Corsica-Sardinia; Ga: Gargano; IS: Ionian Sea; Ist: Istria; LP: Liguro-Provençal Basin; MAR: Mid-Adriatic Ridge; ME: Malta Escarpment; PB: Pannonian Basin; SCRZ: Sicily Channel Rift Zone; SPNF: Shkoder-Peja Normal Fault; TS: Tyrrhenian Sea. Map projection is Transverse Mercator (central meridian 10°E, latitude of origin 43°N)

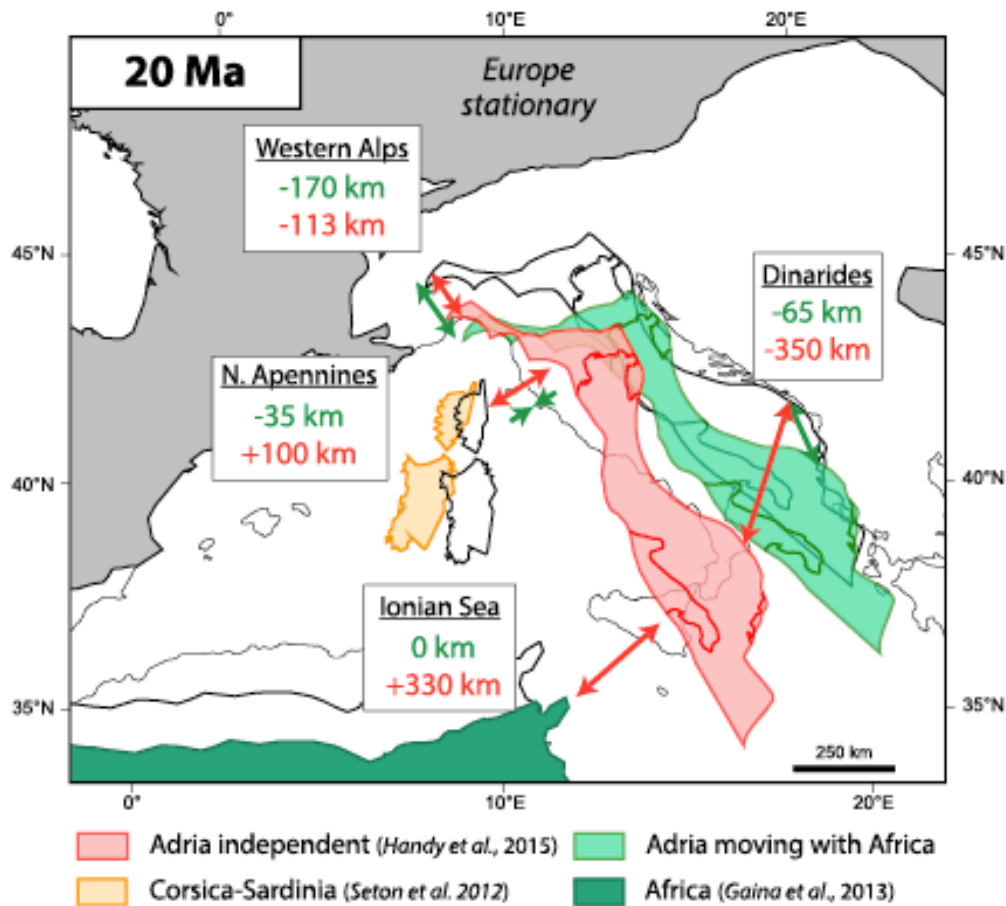


**Figure 2.** Comparison of Adria locations at 20 Ma depending on whether it moved together with Africa (light green) or independently thereof based on data from the Alps (red; Handy et al., 2010; Handy, Ustaszewski, et al., 2015) relative to Europe (gray). Finite Euler rotation poles for Africa (dark green) from Gaina et al. (2013) and Corsica-Sardinia (orange) from Seton et al. (2012). Numbers indicate post-20 Ma overall divergence (+) and convergence (–) in the models. Present-day location of plates and coastline are shown in black. Map projection in Figure 1.

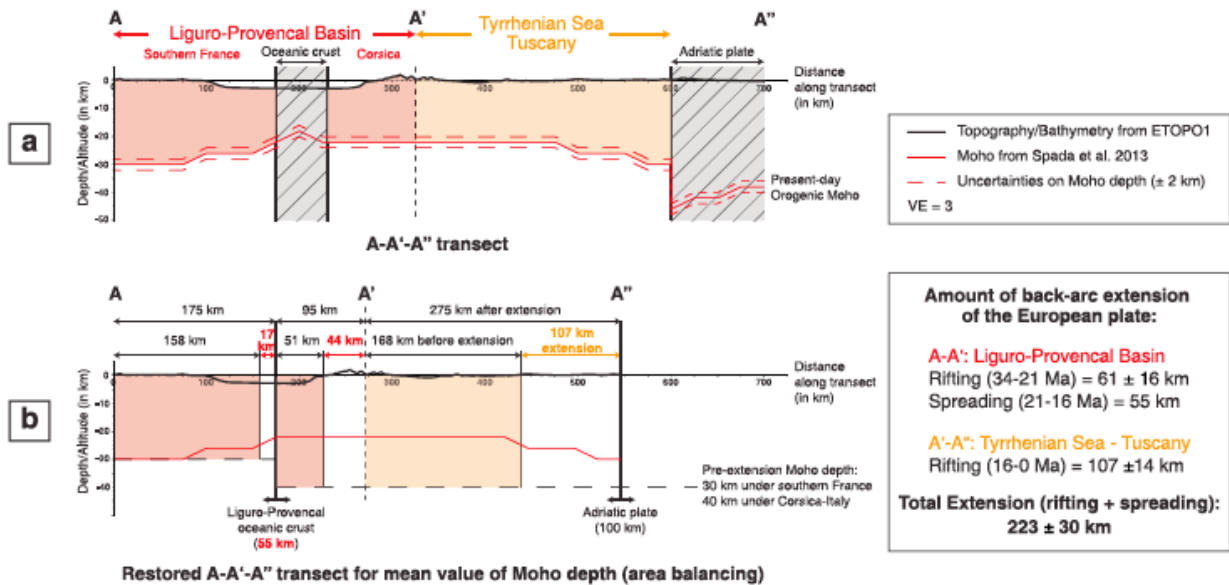


**Figure 3.** (a) Transect A-A'-A'' with Moho depth from Spada et al. (2013), topography/bathymetry from ETOPO1 model (Amante & Eakins, 2009), and width of oceanic crust (55 km, 21–16 Ma) in Liguro-Provençal Basin from Jolivet et al. (2015). Location of transect in Figure 1. (b) Transect A-A'-A'' after areal balancing of the crust shows total extension in Liguro-Provençal and Tyrrhenian Sea. Note that the crust under southern France was restored back to normal thickness (30 km), whereas under Corsica and Italy the crust was restored to an orogenic thickness of 40 km (see text).

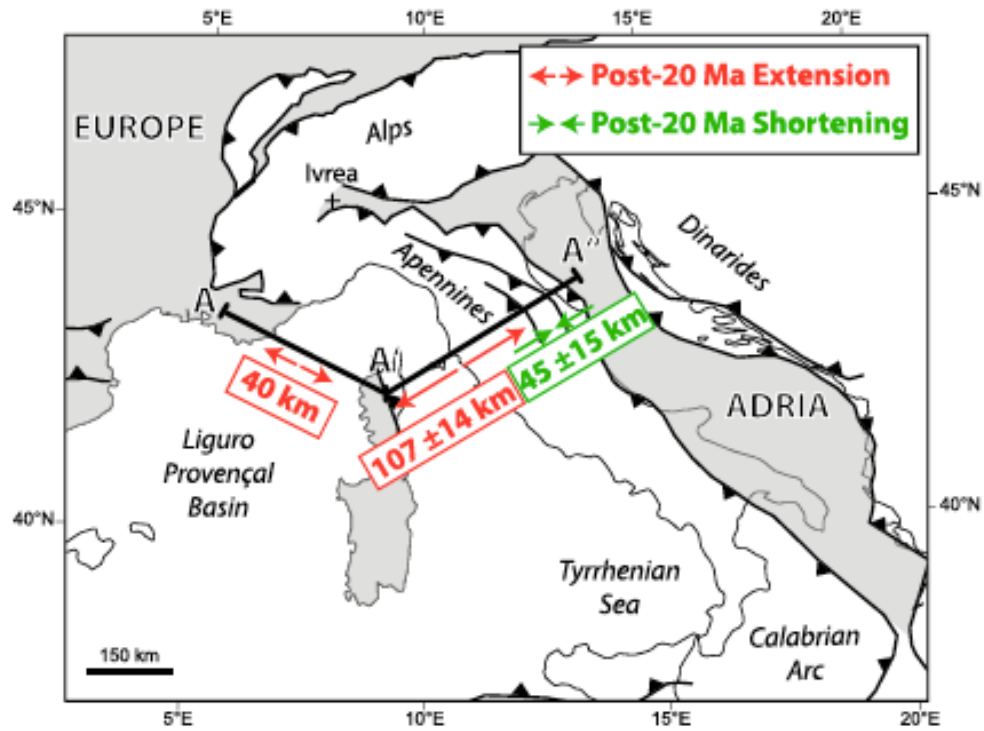


**Figure 4.** Tectonic map of the western Mediterranean showing post-20 Ma extension along transect A-A<sub>0</sub>-A'' in red (Figure 3) and post-20 Ma shortening in the northern Apennines along the CROP03 profile, parallel to transect A<sub>0</sub>-A'', in green (location in Figure 1). Map projection shown in Figure 1.

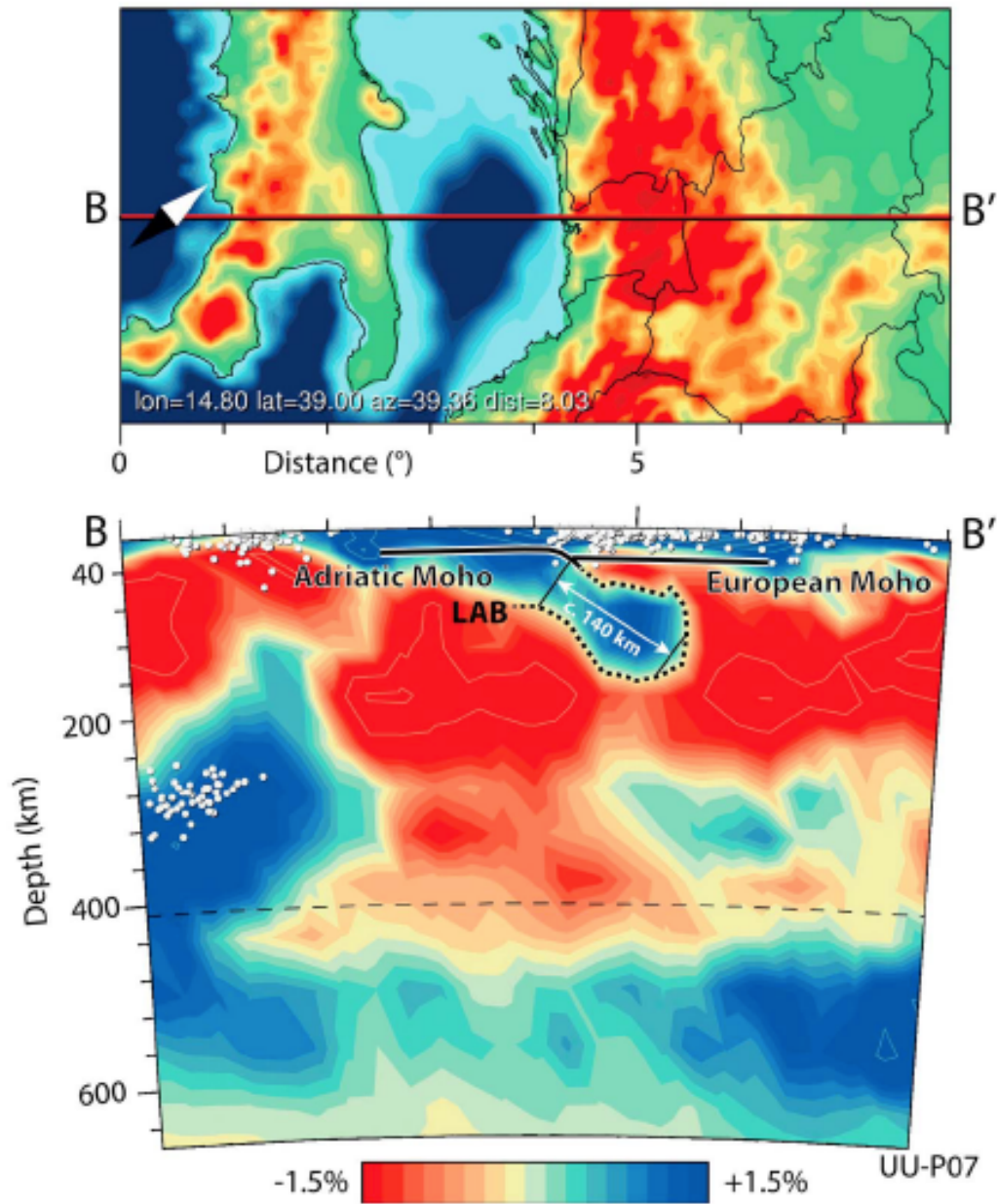


**Figure 5.** P wave tomography (model UU-P07 from Amaru, 2007 and Hall & Spakman, 2015) along transect B-B<sub>0</sub> through the southern Dinarides-Carpatho-Balkan (location in Figures 1 and 6) showing a positive anomaly (blue) interpreted as subducted Adriatic lithosphere. Abbreviation: LAB, Lithosphere Asthenosphere Boundary.

**Table 1**

Compilation of Crustal Shortening, Extension, and Adria-Europe Divergence and Convergence Along Transects A-A', B-B', C-C', and D-D' (Location in Figure 1) Used to Constrain Post-20 Ma Adria Rotation Relative to Europe (R1 and R2 refers to Figure 6)

	Dataset used to determine amount of post-20 Ma Adria rotation	Rotation (R2) for Model 1: 113 km convergence in Western Alps (R1)	Rotation (R2) for Model 2: 60 km convergence in Western Alps (R1)
Liguro-Provençal Basin (A-A')	40 km spreading	Maximum $7.75 \pm 11.75^\circ$ (from $4^\circ$ CW to $19.5^\circ$ CCW)	Maximum $7.25 \pm 11.75^\circ$ (from $4.5^\circ$ CW to $19^\circ$ CCW)
Tyrrhenian Sea-Tuscany (A'-A'')	$107 \pm 14$ km extension assuming 40 km initial thickness $51 \pm 18$ km extension assuming 30 km initial thickness = $33$ – $121$ km divergence		
Northern Apennines (A'-A'')	$30$ – $60$ km shortening assuming thick skinned $100$ km assuming thin skinned = Minimum $30$ – $100$ km convergence		
Southern Dinarides-Carpatho-Balkan (B-B')	$20$ km crustal shortening $140$ km slab length = $20$ – $140$ km convergence	Minimum $0.6^\circ$ CCW; maximum $7^\circ$ CCW	Minimum $0.3^\circ$ CCW; maximum $8^\circ$ CCW
Eastern Alps (C-C')	$115$ – $150$ km convergence	$6.5 \pm 3^\circ$ CCW	$14 \pm 3^\circ$ CCW
Sidly Channel (D-D')	Minimum $30$ km divergence	Minimum $3.5^\circ$ CCW	Minimum $4^\circ$ CCW
Best fit rotation		$5.25^\circ \pm 1.75^\circ$ CCW	No possible fit!

Note. A viable fit of those data is only obtained for Model 1 (involving 113 km convergence in western Alps). More details on calculation of rotations are given in the supporting information.

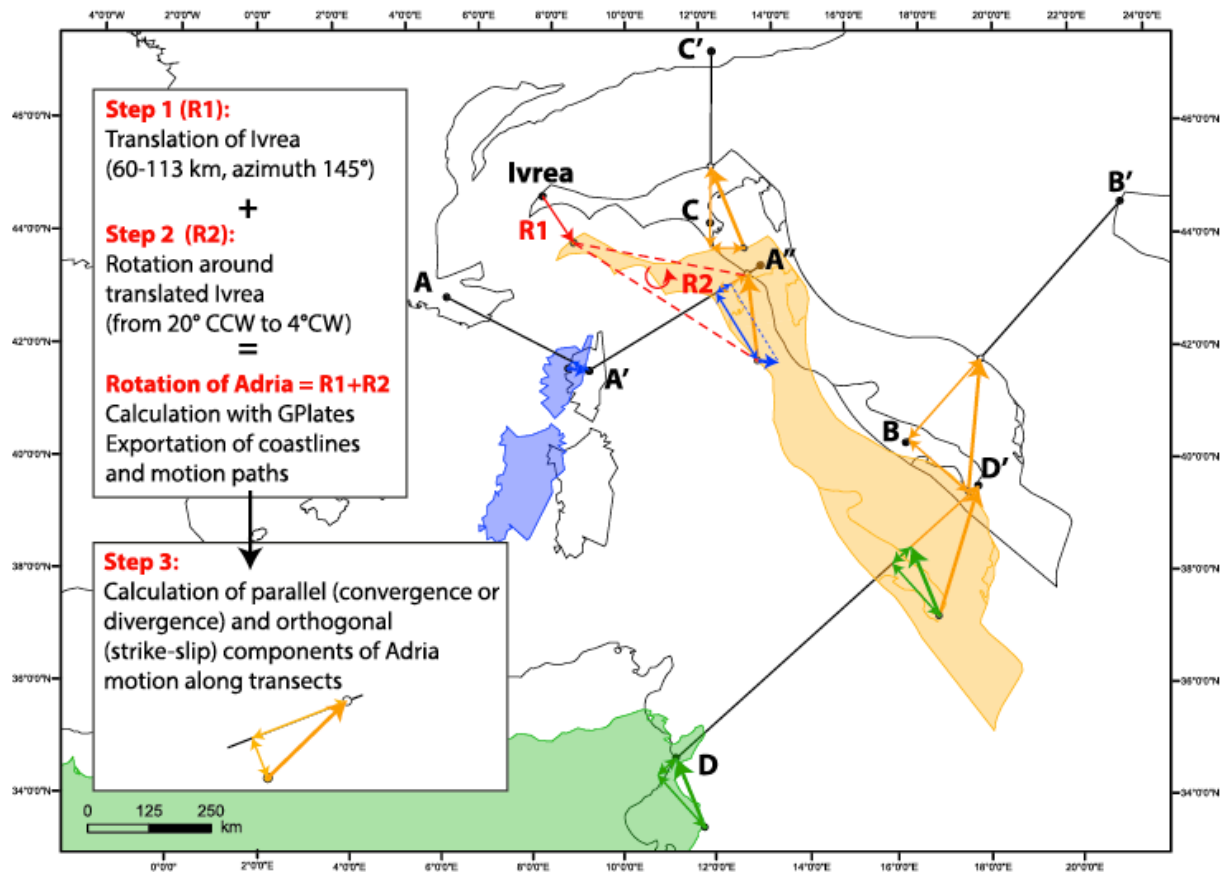


**Figure 6.** Steps for reconstructing post-20 Ma motion path of Adria (yellow) relative to Europe: (1) translate Ivrea to the SE by 113 km (Model 1) or 60 km (Model 2); (2) test different rotations of Adria ( $20^\circ$  CCW to  $4^\circ$  CW) around an axis located at translated Ivrea; and (3) calculate convergence and divergence along transects A-A', B-B', C-C', and D-D' and compare with data set (Table 1). The finite Euler rotation pole (calculated with GPlates) for Adria motion is a combination of Adria translation (R1) and rotation (R2). Post-20 Ma motion of the Corsica-Sardinia block (blue) from Speranza et al. (2002); in compilation of Seton et al., 2012) and of Africa (green) from Gaina et al. (2013) are taken into account when calculating deformation along transect A-A' (blue arrows) and D-D' (green arrows), respectively.



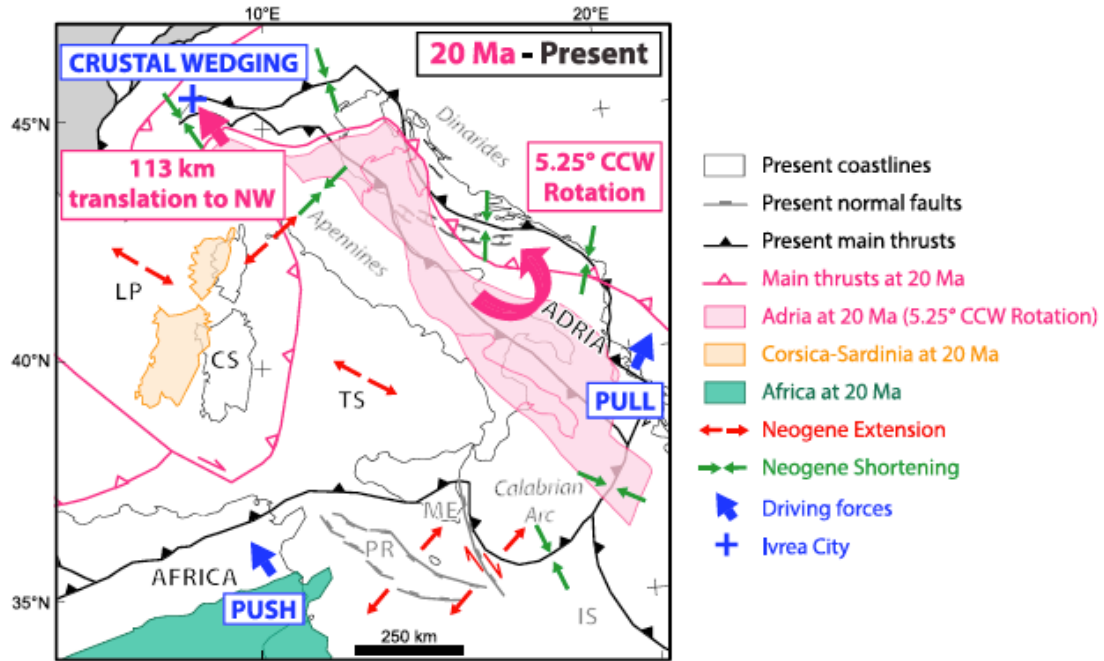


**Figure 7.** Tectonic map of the central Mediterranean region showing location of the Adria microplate and main front thrusts today (black) and at 20 Ma (pink, favored Model 1) relative to Europe. Blue indicates the proposed force vectors driving the motion of Adria (push of Africa from the south, pull of the Adriatic-Hellenic slab to the northeast) during crustal wedging in the Alps that slowed and ultimately stopped Adria NW motion. Note the Neogene NE-SW directed extension along the African margin that has accommodated divergence of Adria and Africa. Abbreviations: CS: Corsica-Sardinia; LP: Liguro-Provençal; ME: Malta Escarpment; PR: Pantelleria Rift; TS: Tyrrhenian Sea. Map projection in Figure 1.